Published OnlineFirst September 28, 2016; DOI: 10.1158/0008-5472.CAN-16-1404

Tumor and Stem Cell Biology

Cancer Research

Recurrent Loss of STING Signaling in Melanoma Correlates with Susceptibility to Viral Oncolysis

Tianli Xia, Hiroyasu Konno, and Glen N. Barber

Abstract

The innate immunoregulator STING stimulates cytokine production in response to the presence of cytosolic DNA, which can arise following DNA damage. Extrinsic STING signaling is also needed for antigen-presenting cells to stimulate antitumor T-cell immunity. Here, we show that STING signaling is recurrently suppressed in melanoma cells, where this event may enable immune escape after DNA damage. Mechanistically, STING signaling was suppressed most frequently by epigenetic silencing of either STING or the cyclic GMP-AMP synthase, which generates STING-activating cyclic dinucleotides after binding cytosolic DNA species. Loss of STING function rendered melanoma cells unable to produce type I IFN and other immune cytokines after exposure to cytosolic DNA species. Consequently, such cells were highly susceptible to infection with DNA viruses including HSV1, a variant of which is being developed presently as a therapeutic oncolytic virus [talimogene laherparepvec (T-VEC)]. Our findings provide insight into the basis for susceptibility to viral oncolysis by agents such as HSV1. *Cancer Res; 76(22); 6747–59.* ©*2016 AACR.*

Introduction

Skin cancer is the most common form of cancer in the United States, and melanoma, affecting about 1.2 million people in the United States, accounts for the vast majority of skin cancer–related deaths. Indeed, the health and economic burden of melanoma is substantial and is projected to increase through 2030 without new interventions (1, 2). Although basal cell and squamous cell skin cancer responds well to treatment, especially if the cancer is detected and cared for early, cutaneous melanomas are usually difficult to treat especially when diagnosed in advanced stages. Melanoma cells commonly exhibit genomic instability and are frequently resistant to conventional chemotherapy and targeted chemo- and immunotherapies (3, 4).

Oncolytic virotherapy is a novel anticancer treatment that generally uses genetically engineered viruses to infect and lyse cancer tissue. Recently, a large variety of RNA- and DNA-based oncolytic viruses (OV) have been tested preclinically and clinically for their ability to exert an oncolytic effect. In many cases, OVs have also been genetically modified to incorporate immunostimulatory modules to enhance systemic antitumor immunity. For example, Amgen talimogene laherparepvec (T-VEC) is a herpes simplex virus type 1 (HSV-1)–based OV that has been engineered to express granulocyte-macrophage colony-stimulating factor (GM-CSF), which may facilitate tumor clearance. It has been recently reported that T-VEC exhibits significant improvement over GM-CSF alone as evaluated in a phase III trials for the treatment of melanoma. However, the overall response rate was noted to remain limited (∼26%; refs. 5, 6). Although OVs have shown potential in cancer treatment including melanoma, these therapeutic strategies are still challenged with safety and effectiveness considerations. Little information is available regarding whether an oncolytic therapy, such as based on HSV1, will exert efficacy in a patient, as the molecular mechanisms explaining viral oncolysis remain to be clarified.

However, considerable information relating to our understanding of antiviral innate immune signaling pathways now exists. For example, stimulator of IFN genes (STING) is an essential molecule that controls the production of host defense proteins, including type I IFNs and proinflammatory cytokine, following the recognition of aberrant DNA species in the cytosol of the cell (7–9). STING is a sensor for cyclic dinucleotides [CDN; cGAMP (c[G(2′,5′)pA(3′,5′)p])] produced by a cellular nucleotidyltransferase referred to as cGAS (cyclic GMP-AMP synthase, Mab-21 domain-containing protein or C6orf150) following its association with nucleic acid species such as viral DNA (10). CDNs such as cyclic di-AMP (c-di-AMP) directly generated by intracellular bacteria are also potent activators of STING-dependent cytokine production (11). Cytosolic DNA species can constitute the genome of invading DNA microbes or even self-DNA leaked from the nucleus or possibly mitochondria (12). Recent studies have shown that STING-dependent cytosolic DNA sensing within phagocytes is essential for the recognition of tumor cells and type I IFN-dependent antitumor immunity (13). It has been observed that loss of STING renders mice susceptible to AOM/DSS-induced colorectal cancer (14). Additional studies have indicated that STING signaling is frequently impaired in human colon cancer cells, an event that might enable such cells to escape immunosurveillance and eradication by phagocytes (15). These data collectively suggest that the STING pathway may have an important function in eliminating transformed cells and for facilitating adaptive antitumor immunity.

Department of Cell Biology and the Sylvester Comprehensive Cancer Center, University of Miami Miller School of Medicine, Miami, Florida.

Note: Supplementary data for this article are available at Cancer Research Online (http://cancerres.aacrjournals.org/).

Corresponding Author: Glen N. Barber, Department of Cell Biology, 511 Papanicolaou Building, 1550 NW 10th Ave, University of Miami Miller School of Medicine, Miami, FL 33136. Phone: 305-243-5914; Fax: 305-243-5885; E-mail: gbarber@med.miami.edu

doi: 10.1158/0008-5472.CAN-16-1404

Published OnlineFirst September 28, 2016; DOI: 10.1158/0008-5472.CAN-16-1404

Given these findings, we have extended our studies into evaluating STING function in melanoma, in part, because such cancers appear to be susceptible to viral oncolytic treatment, which suggests defects in innate immune pathways. Here, we report that STING-mediated innate immune signaling is largely impaired both in human melanoma-derived cells and in primary patient melanoma-derived tissues. We recurrently found loss of STING and/or cGAS expression in melanoma, predominantly through epigenetic hypermethylation silencing. Our findings suggest that suppression of STING signaling may be an important part of tumor development. Moreover, loss of STING function rendered melanoma cells more susceptible to HSV1 and vaccinia virus–mediated oncolysis. Therefore, the development of a prognostic assay that enables the measurement of STING or cGAS expression may lead to a better indication of the efficacy of viral oncolytic treatment.

Materials and Methods

Materials

All reagents were from ThermoFisher Scientific or Sigma unless specified.

Cell culture

Normal human melanocytes (HEMa) and human melanoma cell lines were purchased from and authenticated by ThermoFisher Scientific and ATCC, respectively, in August 2014. hTERT-BJ1 telomerase fibroblasts (hTERT) were purchased from and authenticated by Clontech in 2010.

Immunoblot analysis

Whole-cell lysate was resolved on SDS-PAGE and transferred to polyvinylidene fluoride (PVDF) membranes. After blocking with 5% blocking reagent, membranes were incubated with primary antibodies followed by appropriate secondary antibodies. The image was resolved using an enhanced chemiluminescence system and detected by autoradiography. Antibodies used were: rabbit polyclonal STING antibody (Ishikawa and Barber; ref. 8), β-actin (Sigma Aldrich), p-IRF3 (Cell Signaling), IRF3 (Santa Cruz Biotechnology), p-p65 (Cell Signaling), p65 (Cell Signaling), p-TBK1 (Cell Signaling), TBK1 (Abcam), and cGAS (Cell Signaling).

IFNβ ELISA analysis

IFNβ ELISA was performed using the Human IFNβ ELISA Kit (PBL InterferonSource) following the manufacturer's protocol.

Immunofluorescence microscopy

Cells were cultured and treated with glass coverslips. Cell were fixed with 4% paraformaldehyde for 15 minutes at 37°C and permeabilized with 0.05% Triton X-100 for 5 minutes at room temperature. Immunostaining was performed with rabbit-anti-STING polyclonal, rabbit-anti-IRF3 (Santa Cruz Biotechnology), or rabbit-anti-p65 (Cell Signaling) followed by fluorescence-conjugated secondary antibodies (FITC goat-anti-rabbit). Images were taken with Leika LSM confocal microscope at the Image Core Facility, University of Miami (Miami, FL).

Quantitative real-time PCR

Total RNA was reverse-transcribed using QuantiTect Reverse Transcription Kit (Qiagen). Real-time PCR was performed with the TaqMan gene Expression Assay (Applied Biosystems).

Immunohistochemistry and histologic analysis

Tissue microarray was purchased from Pantomics. Immunohistochemical (IHC) staining was performed with rabbit-anti-cGAS antibody or rabbit-anti-STING antibody following standard protocol.

Virus amplification, purification, titration, and infection

HSV-1 γ34.5 was kindly provided by Bernard Roizman. Vaccinia virus (vTF7-3) was kindly provided by John Rose. Virus was amplified in Vero cells and purified by sucrose gradient ultracentrifugation following standard protocol. Plague assay using serial diluted virus was performed in Vero cells following standard protocol. Cells were infected with virus at specific multiplicity of infection (MOI) for 1 hour, washed, and then incubated for designated period for specific assay examination.

RNA *in situ* hybridization

STING and cGAS RNA probed was custom-designed by ACD and RNA *in situ* hybridization (RNAish) was performed using RNAscope Multiplex Fluorescent Reagent Kit for cultured cells and 2-plex RNAscope Reagent Kit for formalin-fixed, paraffin-embedded (FFPE) cells and tissue following the manufacturer's instruction.

Mouse treatment

Balb/C *nu*/*nu* mice were purchased from Charles River and maintained in the institutional Division of Veterinary Resources. All experiments were performed with Institutional Animal Care and Use Committee (IACUC) approval and in compliance with IACUC guidelines. Tumor cells were introduced in the flanks of Balb/c nude mice by subcutaneous injection of $2E10^6$ of the appropriate tumor cells and tumors allowed to develop to an average diameter of approximately 0.5 cm. HSV1γ34.5 was then injected into the tumors every other day for a total of 3 times at 1E7 PFU. PBS was used as vehicle control. Effects on tumor growth were monitored. Mice were euthanized when tumor diameter exceeds 10 mm.

gDNA sequencing

gDNA was extracted from melanoma cells as well as normal cells using Qiagen DNeasy Kit, and specific locus was sequenced by Polymorphic DNA Technologies.

Statistical analysis

All statistical analysis was performed by the Student *t* test unless specified. The data were considered to be significantly different when $P < 0.05$.

Results

Recurrent loss of STING signaling in human melanoma-derived cell lines

The STING-controlled innate immune pathway has been reported to be largely impaired in human colon cancers, an event that may facilitate tumorigenesis (15). To evaluate whether this key pathway is similarly defective in other types of cancer, we further examined STING expression by immunoblot in a panel of human malignant melanomas. These results showed that STING expression was not detectable in 3 of 11 cell lines examined (G361, MeWo, and SK-MEL-5), and STING expression level was dramatically suppressed in a further 3 cell lines (SK-MEL-

Published OnlineFirst September 28, 2016; DOI: 10.1158/0008-5472.CAN-16-1404

2, SK-MEL-28, and WM115; Fig. 1A). The synthase cGAS resides upstream of STING and generates CDN's capable of triggering STING function. We therefore complemented this study by similarly examining the expression of cGAS by immunoblot and found that this synthase was absent in 4 of 11 cell lines examined (A375, G361, SK-MEL-5, and SK-MEL-24; Fig. 1A). Real-time PCR analysis using cGAS probe confirmed that *cGAS* was not detectable in A375 and SK-MEL-5, but low level of *cGAS* was detected in G361 and SK-MEL-24 (Fig. 1A). Immunoblot analysis using higher amount of whole-cell lysate further confirmed cGAS expression in G361 cells albeit at low level (Supplementary Fig. S3C). To correlate STING/cGAS expression analysis with functional STING signaling, we next transfected cells with dsDNA to activate STING-dependent cytokine production or with dsRNA (polyI:C) to activate the STING-independent RIG-I like signaling pathway and measured type I IFN expression by ELISA (7). This study indicated that all 11 melanoma cells responded poorly to STING-dependent, dsDNA-triggered type I IFN production. Using fluorescent microscopy analysis, we confirmed that all cells were indeed transfected with fluorescein isothiocyanate (FITC)-labeled dsDNA activator (Supplementary Fig. S1). However, control hTERT cells and normal HEMa were able to express high levels of IFNβ when transfected with dsDNA, suggesting the STING-mediated type I IFN responses were suppressed specifically in the melanoma cells (Fig. 1B). This finding was further supported by real-time PCR analysis, in which dsDNA stimulated *IFNB* and *CXCL10* induction was suppressed in majority of the

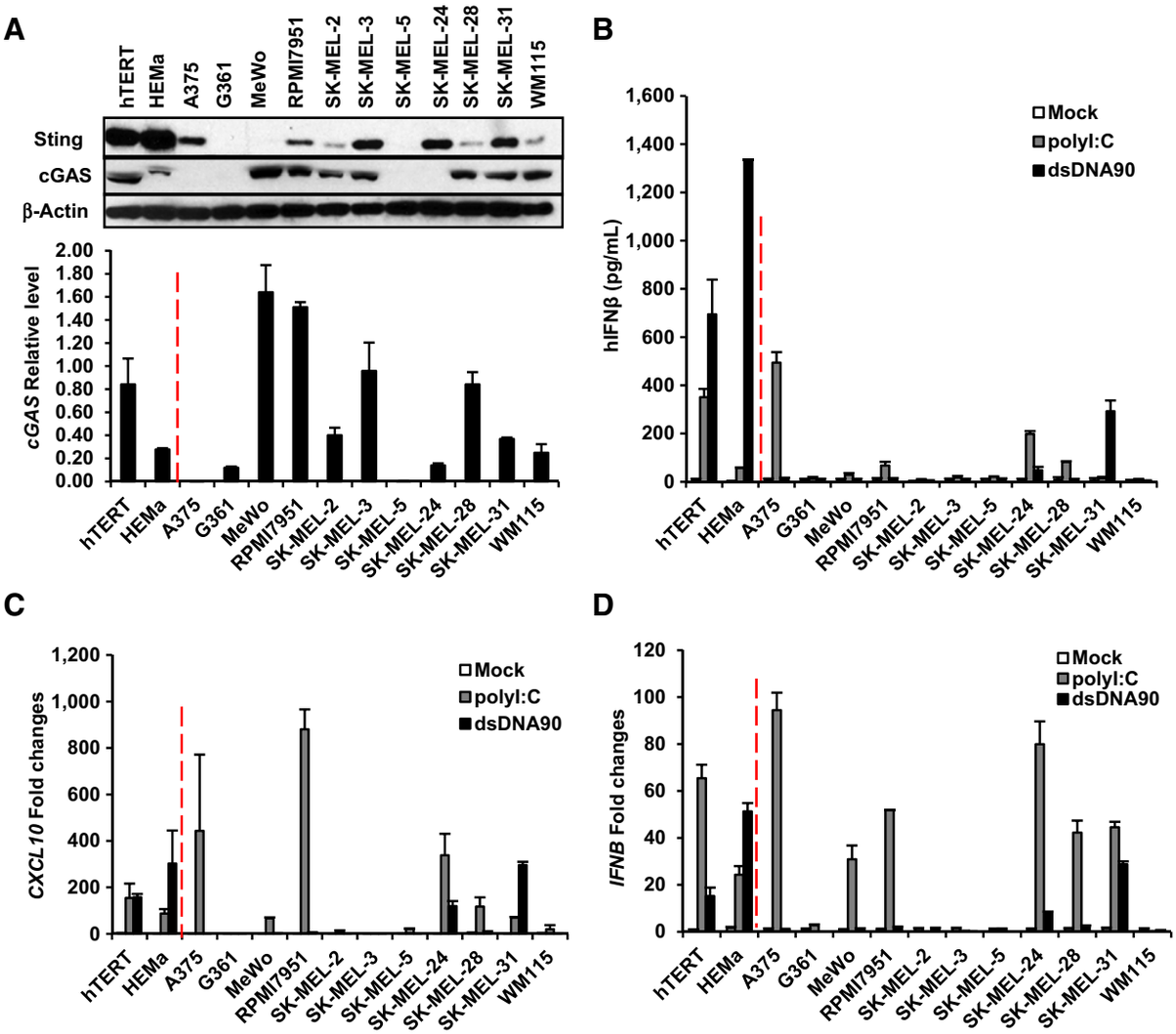

Figure 1.

STING expression is suppressed and dsDNA-induced innate immune activation is impaired in majority of human melanoma cell lines. **A,** hTERT fibroblasts, normal HEMa, and a series of human melanoma cell lines were analyzed for STING and cGAS expression by immunoblot at 20 μg whole-cell lysate input (top). β-Actin was analyzed as loading control. *cGAS* expression was also analyzed by qPCR (bottom). **B,** ELISA analysis of human INFβ production in the media of cells (same as **A**) transfected with 3 μg/mL polyI:C or dsDNA90- or mock-transfected for 16 hours. qPCR analysis of human *CXCL10* (**C**) and *IFNB* (**D**) induction in cells (same as **A**) transfected with 3 μg/mL dsDNA90- or mock-transfected for 3 hours.

Published OnlineFirst September 28, 2016; DOI: 10.1158/0008-5472.CAN-16-1404

melanoma cells examined, although weak activity was detected in SK-MEL-24 and SK-MEL-31 cells (Fig. 1C and D). In contrast, 6 of the 11 melanoma cells were able to produce type I IFN and CXCL10, albeit at various levels, in response to dsRNA, indicating that the RIG-I–like RNA signal pathway were mostly intact in majority of melanoma cells examined (Fig. 1B–D). Using siRNA treatment to knockdown STING expression in normal cells and 2 melanomas cell lines (SK-MEL-24, SK-MEL31) that appeared to retain partial STING activity, we confirmed that the upregulation of these dsDNA-induced cytokines was STING-dependent (Supplementary Fig. S2). Taken together, our data indicate that STING-dependent signaling is largely impaired in a majority of melanoma cells with only SK-MEL-24 and SK-MEL-31 exhibiting weak STING activity. Furthermore, the chemotherapy drug cisplatin triggered *IFNB* and *CXCL10* induction in normal hTERT and melanoma SK-MEL-31 cells with functional STING signal, but not in melanoma cells lacking STING activity (A375, G361, MeWo, and SK-MEL-5), suggesting that STING signal is required for cytokine production in cancer cells following DNA damage, an event that may alert immune system for and facilitate antitumor responses (Supplementary Fig. S3A and S3B).

Loss of STING-dependent TBK1-IRF3 activation in melanoma cells

To examine the extent of STING signaling defect in melanoma cells, we evaluated IRF3 and NF-κB activation by immunofluorescent microscopy and immunoblot analysis. When stimulated with dsDNA, STING rapidly undergoes translocation from the endoplasmic reticulum (ER), along with TBK1, to perinuclear-associated endosomal regions, containing NF-κB and IRF3, in a procedure similar to autophagy (7, 16). This incident accompanies STING phosphorylation and degradation, almost certainly to avoid prolonged STING-induced cytokine production, which is now known to provoke chronic inflammation (17). Our results confirmed that, following dsDNA treatment in normal hTERT cells, STING translocated to perinuclear region and underwent phosphorylation and degradation events (Fig. 2A and D, left). During this process, TBK1 was phosphorylated in hTERT cells as well as its cognate target IRF3 and the p65 subunit of NF-κB (Fig. 2D). We also observed IRF3 and p65 translocation into the nucleus, indicating normal activation (Fig. 2B–D). A similar effect was observed in SK-MEL-24 and SK-MEL-31 cells, which exhibited partial dsDNA-dependent cytokine production, confirming that these 2 cell lines retained some STING function (Figs. 2A–D and 1B–D). However, while RPMI7951 and SK-MEL-3 retained STING/cGAS expression and displayed similar IRF3 activation upon dsDNA treatment, these cells lacked p65 translocation. This observation would explain why dsDNA failed to trigger type I IFN production, which requires both IRF3 and NF-κB for its transcriptional activation (Figs. 2A–D and . 1B–D). In addition, in cells where STING and/or cGAS expression were not detected (such as A375, G361, MeWo, and SK-MEL-5), no evidence of TBK1 or IRF3 phosphorylation/translocation was detected in these cells following dsDNA treatment (highlighted by red boxes; Fig. 2B and D). Although phosphorylated p65 was observed, no translocation of this transcription factor into the nucleus was evident in any of the RPMI7951, SK-MEL-3, A375, G361, MeWo, or SK-MEL-5 cells (Fig. 2C and D). These results indicate that dsDNA-induced STING signaling is deregulated at various points along the pathway in many of the melanoma cell lines examined (Fig. 2 and Supplementary Fig. S4). For example, while STING retained some signaling activity and ability to induce the translocation of IRF3, as in RPMI7951 and SK-MEL-3 cells, NF-κB signaling was observed to be affected. In contrast, STING did not appear to undergo any phosphorylation or translocation in A375, G361, MeWo, or SK-MEL-5 cells, suggesting that STING function is affected upstream of IRF3/NF-κB activation, likely due to loss of STING and/or cGAS expression.

RNAscope and IHC analysis of STING/cGAS expression

Since the STING pathway requires the presence of STING and cGAS, and since STING and/or cGAS expression was observed to be absent in about 40% melanoma cells examined, being able to measure the presence of STING and cGAS could be useful in predicting functional STING signaling in melanoma. Although immunoblot and RT-PCR methodology is effective in examine STING/cGAS expression in cultured cell lines, biopsied tissue often contains not only tumor cells but also other cell types including infiltrating immune cells that could retain normal STING/cGAS expression (9). Thus, analysis of STING and/or cGAS protein or RNA expression within the cancer cell itself is necessary for accurate evaluation into the presence of these products. We previously developed an RNAish assay using RNAscope technology that can efficiently detect *STING*/*cGAS* mRNA copies within individual cells. By using FITC-labeled STING probe (green) and Cy5-labeled cGAS probe (red), we similarly examined melanoma cells using RNA FISH. Results showed that both probes combined within the same assay effectively detected *STING* and *cGAS* mRNA in control HEMa cells. *STING* mRNA (green) was also detected in A375, SK-MEL-24, and SK-MEL-31 cells but not in G361, MeWo, or SK-MEL-5 cells whereas, *cGAS* mRNA (red) was not detected in A375 or SK-MEL-5 cells (Fig. 3A). mRNA copy numbers were quantitated with results being consistent with our previous results obtained using our expression analysis (Figs. 1A and 3A). Thus, RNA FISH analysis can effectively quantitate STING/cGAS expression simultaneously in single cells.

We further evaluated mRNA expression by chromogenic *in situ* hybridization (RNA CISH) of paraffin-embedded melanoma cells. This situation may mimic situations where biopsied and paraffin-embedded patient-derived materials are generally used for biomarker analysis. This study indicated that we were able to detect and quantitate both *STING* and *cGAS* mRNA expression in SK-MEL-24 and SK-MEL-31 cells as before. In A375 cells, only *STING* was detected, whereas *cGAS* was absent. *STING* was not detected in G361 or MeWo cells. Both *STING* and *cGAS* were absent in SK-MEL-5 cells (Fig. 3B). Overall RNA CISH analysis generated results similar to RNA FISH evaluation.

Using antibody to cGAS and STING, we also performed IHC analysis on paraffin-embedded cells and confirmed cGAS and STING protein expression status in accord with our immunoblot and RNAscope studies (Fig. 3C).

IHC analysis of STING/cGAS expression in melanoma tissue microarray

To evaluate STING/cGAS expression in patient-derived melanoma samples, we subsequently examined by IHC analysis a paraffin-embedded melanoma tissue microarray (TMA; MEL961, Pantomics) that contains 8 normal skin tissues, 8 benign nevus tissues, 56 malignant melanoma tissues, and 24 metastatic

Published OnlineFirst September 28, 2016; DOI: 10.1158/0008-5472.CAN-16-1404

melanoma tissues. We observed that all normal tissues expressed both STING and cGAS. cGAS was not detected in 2 benign nevus tissues, whereas STING was noted to be present in all 8 nevi. In malignant melanoma tissues, 23.2% of melanoma samples lost STING expression, whereas 16.1% of melanoma samples did not express cGAS, and both STING and cGAS were absent in 14.3% of melanoma tissues. In more advanced metastatic melanoma tissue, loss of both STING and cGAS was more profound (41.7%; Fig. 4 and Supplementary Table S1). Given these data, suppression of STING or cGAS expression may commonly occur in human melanoma and plausibly other human cancers (15). In summary, our IHC procedures may be useful for the analysis of cGAS and STING expression in FFPE preserved clinical tumor samples.

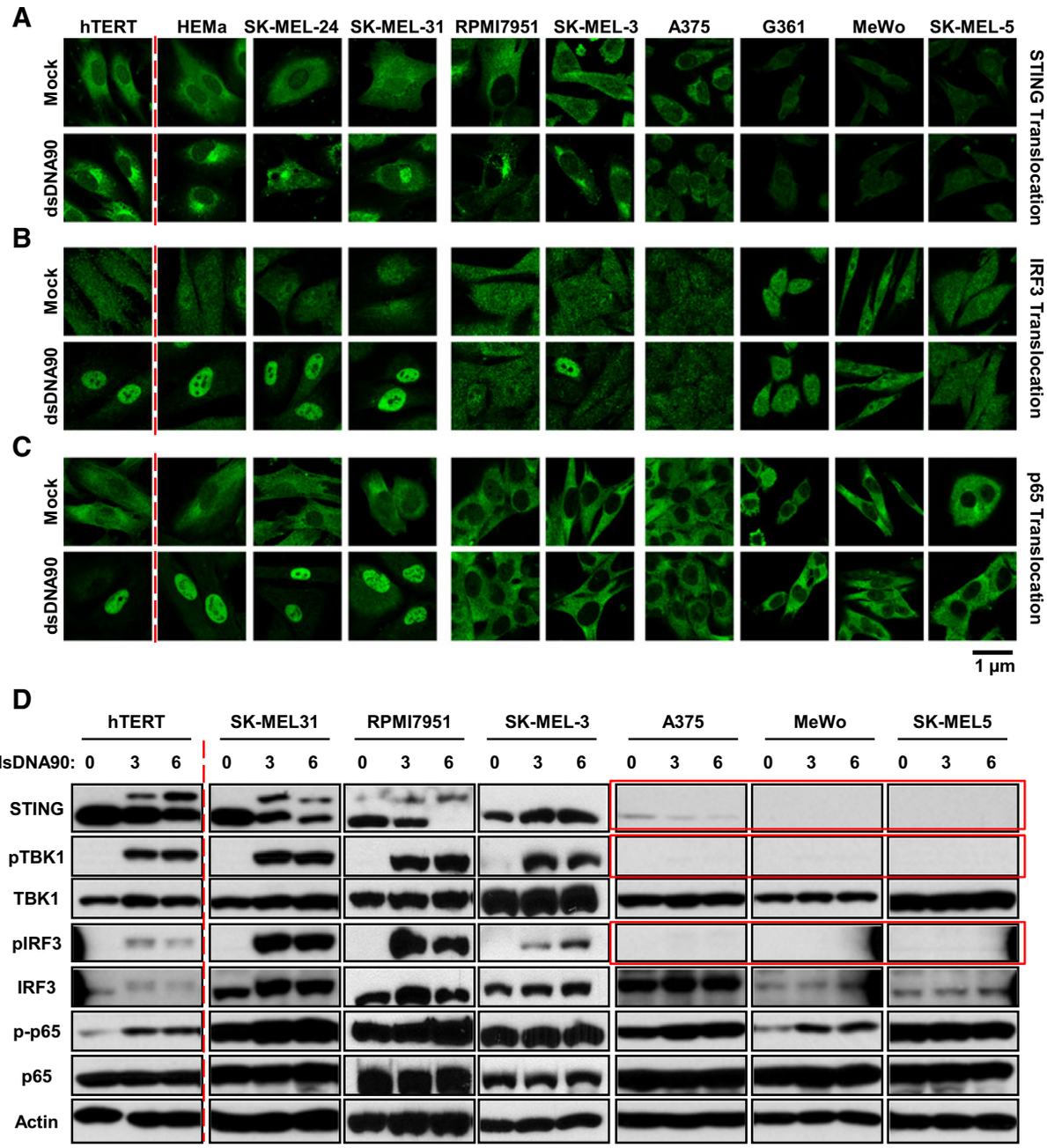

Figure 2.

dsDNA-induced STING signaling pathway is defective in majority of human melanoma cell lines. Immunofluorescent microscopy analysis of STING translocation (**A**), IRF3 translocation (**B**), and p65 translocation (**C**) in normal and human melanoma cell lines transfected with 3 μg/mL dsDNA90- or mock-transfected for 3 hours. Original magnification, ×1,260; bar size, 1 μm. **D,** immunoblot analysis of STING signal activation in cells (same as above) transfected with 3 μg/mL dsDNA90 for indicated time periods.

Published OnlineFirst September 28, 2016; DOI: 10.1158/0008-5472.CAN-16-1404

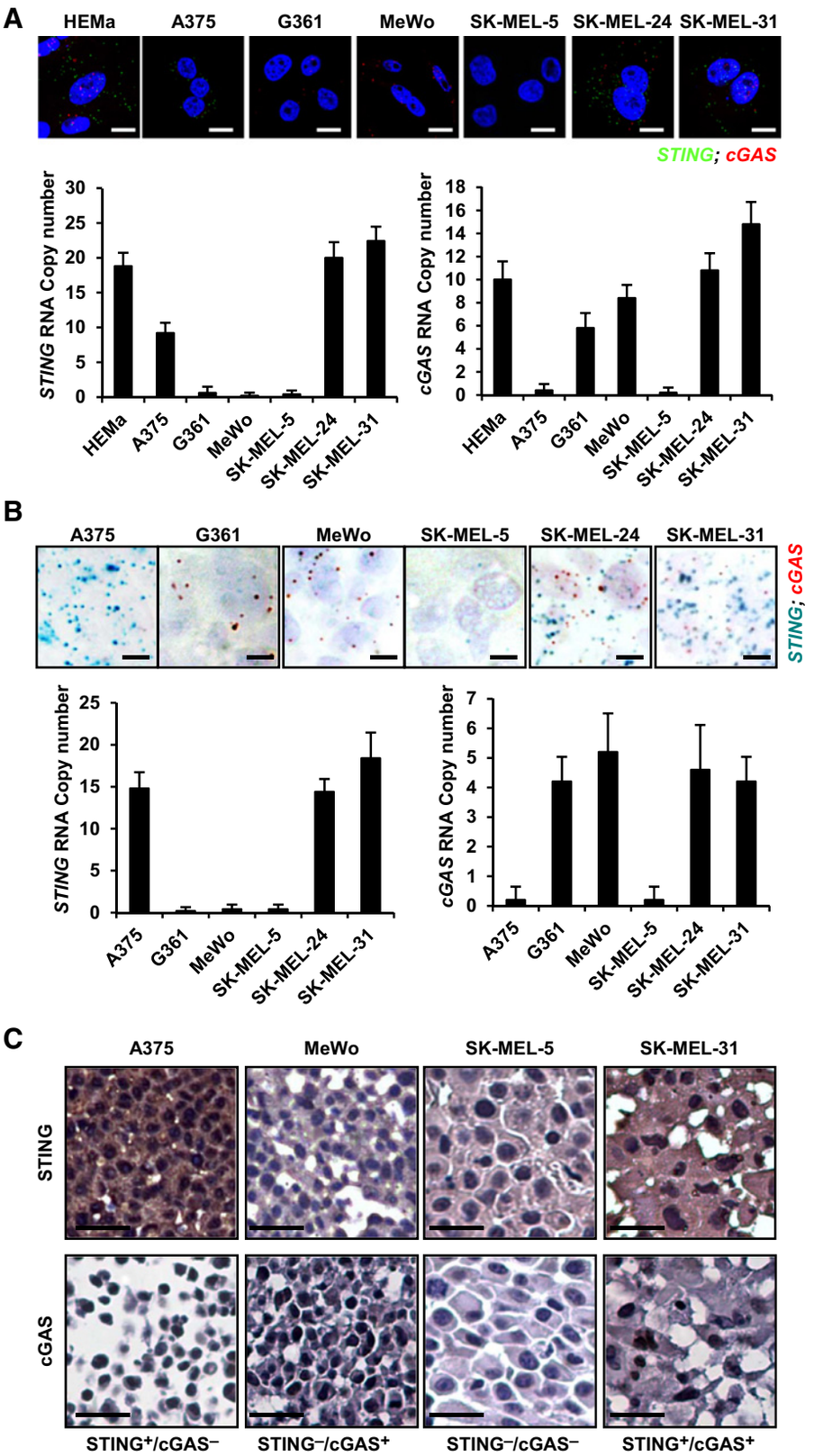

Figure 3.

RNAish and IHC analysis of STING and cGAS in human melanoma cell lines. **A,** RNA FISH analysis of STING and cGAS expression in normal and human melanoma cell lines. Representative images are shown at ×1,260. Bar size, 500 nm. Quantitation of *STING* and *cGAS* RNA copy numbers are shown in bar graph. **B,** RNA CISH analysis of STING and cGAS expression in FFPE normal and human melanoma cell lines. Representative images are shown at ×600. Bar size, 1 μm. quantitation of *STING* and *cGAS* RNA copy numbers are shown in bar graph. **C,** IHC analysis of STING and cGAS expression in melanoma cells. Images were shown at ×400. Bar size, 20 μm.

Published OnlineFirst September 28, 2016; DOI: 10.1158/0008-5472.CAN-16-1404

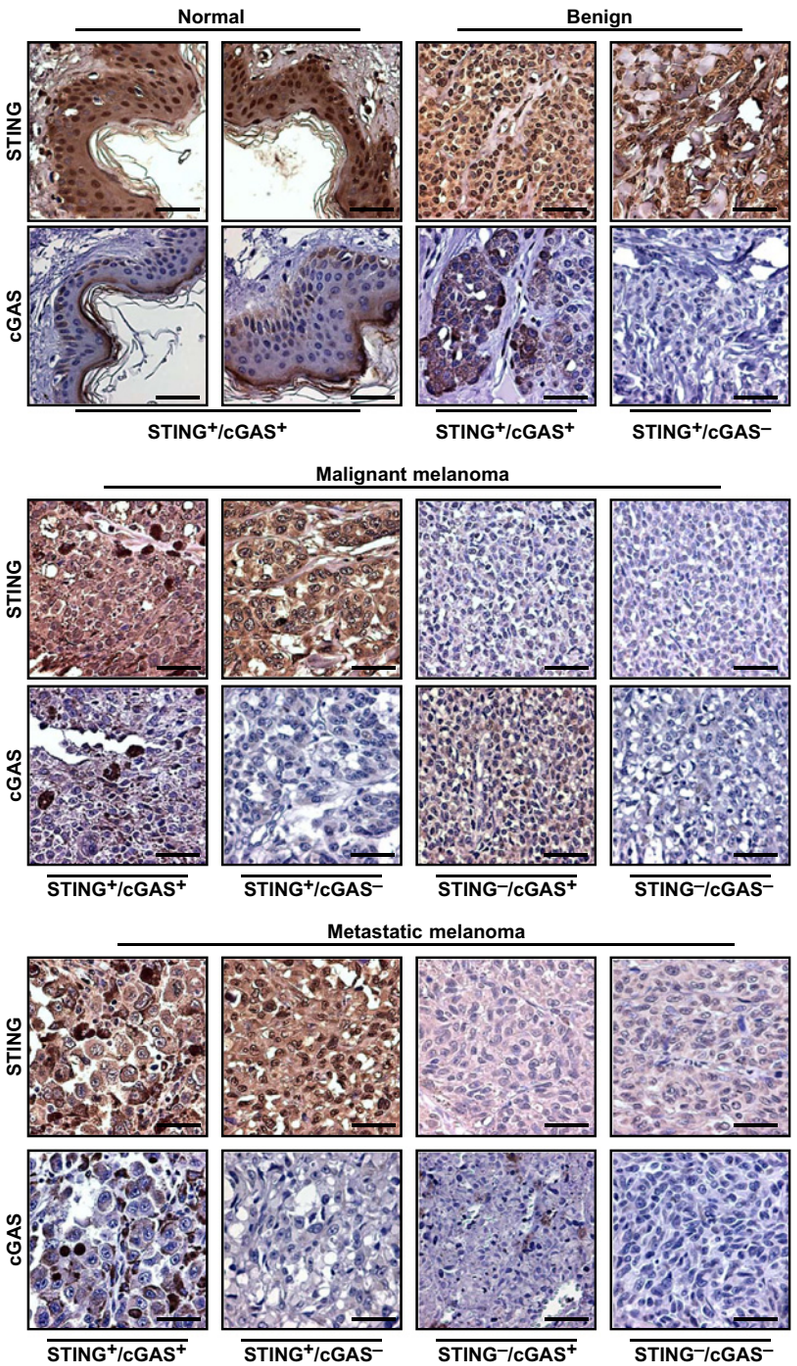

	Normal	Benign	Malignant	Metastatic
STING+/cGAS+	100% (8/8)	75% (6/8)	46.4% (26/56)	37.5% (9/24)
STING−/cGAS+			23.2% (13/56)	8.3% (2/24)
STING+/cGAS−		25% (2/8)	16.1% (9/56)	12.5% (3/24)
STING−/cGAS−			14.3% (8/56)	41.7% (10/24)

Figure 4.

STING and cGAS expression were suppressed in high percentage of human melanomas. IHC analysis of STING and cGAS in human melanoma TMA containing normal human epidermal and human melanoma tissues. Representative images of normal human epidermal and human melanoma tissues stained for STING and cGAS. Images are shown at ×400. Bar size, 50 μm. STING and cGAS expression status is summarized and shown in the bottom.

Published OnlineFirst September 28, 2016; DOI: 10.1158/0008-5472.CAN-16-1404

STING/cGAS expression may be suppressed through DNA hypermethylation in melanoma cells

Loss of STING/cGAS expression could occur through either genetic alteration or mutation. To evaluate the gene status of *STING* and *cGAS* in melanoma cells, we sequenced the *STING* and *cGAS* gene within all 11 melanoma cells. Sequence analysis of the entire *STING* gene (introns and exons comprise approximately 7.2 kb on chromosome 5q31.2) indicated that 7 of the 11 melanoma cells exhibited HAQ STING variant (18, 19), which was previously reported to occur in approximately 20% of the population (Supplementary Table S2). *STING* gene in all melanoma cells as well as normal HEMa cell contains the R272 polymorphism, which was reported to represent approximately 85% of the population but does not exert any defects in STING function (Supplementary Table S2). Collectively, sequence analysis did not reveal any major genetic defect in the *STING* gene within the melanoma cells. Similar sequence analysis was also carried out on *cGAS* exons. However, no major mutations or deletions were noted (Supplementary Table S3). Taken together, genetic mutations or deletions do not seem to be involved in STING/cGAS defective expression in melanoma cells. In view of this, we examined whether STING or cGAS expression was suppressed by epigenetic processes, such as by hypermethylation of the promoter regions (20, 21). Indeed, databank analysis indicated the presence of considerable CpG islands within the *STING* and *cGAS* promoter region (Supplementary Fig. S5). We thus treated melanoma cells lacking either STING or cGAS expression with the demethylating agent 5-aza-2′-deoxycytidine (5AZADC) for 5 days and evaluated recapitulation of STING or cGAS expression. Real-time PCR analysis showed that *cGAS* expression was recovered in A375 cells as well as SK-MEL-5 cells, although at a lower extent. Although SK-MEL-24 exhibited low *cGAS* expression by RT-PCR, 5AZADC treatment did not seem to affect *cGAS* expression level of SK-MEL-24 cells significantly (Fig. 5A). This result was again confirmed by both immunoblot and RNA FISH analysis, in which cGAS expression was apparently recapitulated in A375 and SK-MEL-5 cells following 5AZADC demethylation (Fig. 5B and C). In MeWo cells, STING expression was restored by 5AZADC treatment as shown by both immunoblot and RNA FISH analysis. However, STING remained absent in similarly treated G361 cells as well as in SK-MEL-5 cells, although cGAS expression was partially restored in the same treated SK-MEL-5 cells (Fig. 5A–C). Therefore, DNA hypermethylation is involved in silencing STING or cGAS expression in some melanoma cells (A375 and MeWo). However, it is not yet clear why expression levels of STING are muted in the remainder melanoma cells (G361, SK-MEL-5). Other epigenetic modifications such as histone modifications or other transcription regulator factors such as miRNA could be involved in suppressing STING and/or cGAS expression (22, 23). To determine whether reconstitution of STING/cGAS expression rescued STING-dependent dsDNA signaling, we examined *IFNB* and *CXCL10* induction in 5AZADC-treated melanoma cells following dsDNA stimulation. We observed induction of both *IFNB* and *CXCL10* production in cGAS rescued A375 cells, as well as modest expression of *IFNB* in STING rescued MeWo cells, concomitant with IRF3 and STING translocation (Fig. 5D–G). Whereas no STING function was observed in G361 or SK-MEL-5 cells following 5AZADC treatment, we confirmed that both STING and cGAS are necessary for dsDNA-stimulated cytokine production (Fig. 5D and E). Thus, demethylating agents may be able to partially rescue STING-dependent innate immune gene induction in select melanoma cells.

Defect in STING signal renders melanoma cells susceptible to DNA virus infection

STING innate immune signaling plays a critical role in host defense responses to DNA viruses. For example, mice lacking STING are extremely sensitive to HSV infection (7, 9). A strain of HSV1 lacking the γ34.5 gene, referred to as talimogene laherparepvec (OncoVex, T-VEC), is presently being evaluated in clinical trials as a therapeutic agent for the treatment of cancer including melanoma (5, 6, 24). However, the mechanisms of oncolysis remain to be fully determined and there is no evaluation, presently, for determining the likely efficacy of HSV-based antitumor treatment. We have previously shown that STING activity is defective in numerous colon cancer cells, which renders cells sensitive to DNA virus infection including HSV1. We postulated that lack of STING function in melanomas cells may correlate with an increased susceptibility to DNA virus infection and replication. Plausibly, the ability of STING to effectively signal may affect outcome to HSV-based oncoviral therapy. To start addressing this, we infected the melanoma cells or control hTERT and HEMa with HSV1 lacking the γ34.5 gene similar to the strain presently being investigated as an oncolytic agent against human melanoma. The γ34.5 viral protein has been proposed to suppress host defense responses, although the mechanisms need to be fully clarified. Thus, without the robust repression of the host innate immune signaling, HSV1γ34.5 is able to potently trigger STING-dependent innate immune activation, including type I IFN production (9). Similar to dsDNA treatment, HSV1γ34.5 induced robust production of *IFNB* and *CXCl10* mRNAs in control hTERT and HEMa cells, as well as in SK-MEL-24 and SK-MEL-31 cells that retained partial STING signaling (Fig. 6A and B). However, little type I IFN production was observed in the remainder of the melanoma cells. Loss of the ability to induce type I IFN correlated with increased HSV1γ34.5 replication, likely due to the impaired antiviral effects, especially in melanoma cells lacking STING/cGAS expression (A375, G361, MeWo, and SK-MEL-5; Fig. 6C). Furthermore, cells with defective STING signal underwent rapid cell death, likely due to robust viral replication, whereas control cells and cells with partial STING function (SK-MEL-24 and SK-MEL-31) were significantly more resistant (Fig. 6D). These data confirmed that melanoma cells exhibiting defective STING-signaling enabled more HSV1 replication and lysis. We further examined the ability of vaccinia virus to activate host innate immune signaling in the absence of STING function in melanoma cells. Vaccinia virus, a dsDNA virus with 190-kb genome that replicates in the cytoplasm of infected cells, is another candidate DNA virus that is currently under evaluation as an oncolytic therapeutic agent to treat cancer (25). Similar to our observations using HSV1γ34.5, vaccinia virus triggered *IFNB* and *CXCL10* production only in the control cells and melanoma cells with partial STING function but not in cells with loss of STING/cGAS expression (A375, G361, MeWo, and SK-MEL-5; Supplementary Fig. S6). Our results indicate that melanoma cells with defective STING signaling are highly susceptible to HSV1 and vaccinia virus infection. Thus, it is plausible that melanoma lacking STING/cGAS expression is more sensitive to DNA virus oncolytic activity and being able to measure STING/cGAS expression in melanoma tissue may help predict the response of patients to selected viral oncolytic therapy.

Published OnlineFirst September 28, 2016; DOI: 10.1158/0008-5472.CAN-16-1404

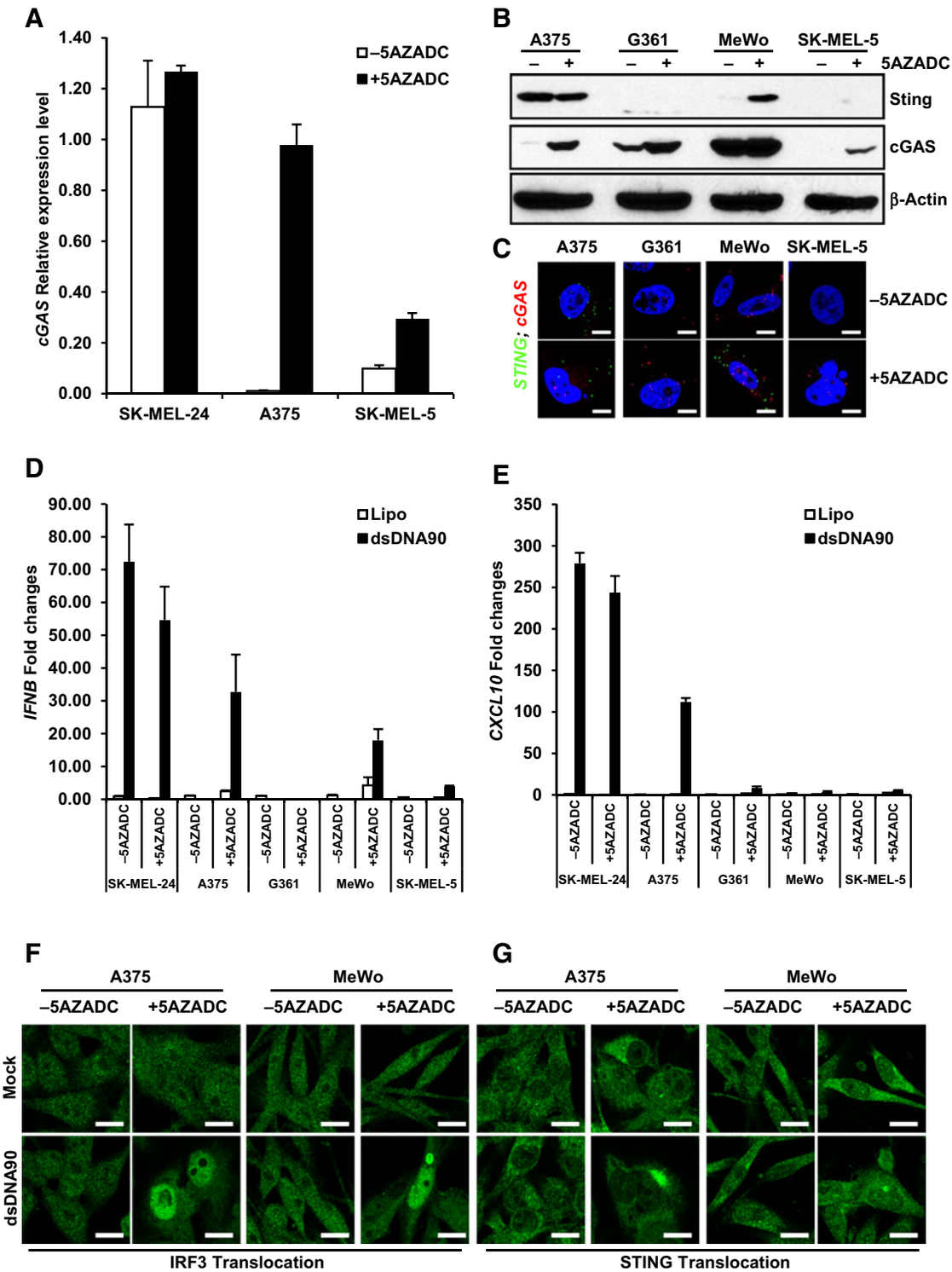

Figure 5.

DNA demethylation partially recapitulated STING and cGAS expression in human melanoma cell lines. **A,** qPCR analysis of *cGAS* expression in indicated human melanoma cells mock-treated or treated with 1 μmol/L 5AZADC for 5 days. **B,** immunoblot analysis of STING and cGAS in indicated human melanoma cells treated same as above. Fifty micrograms of whole-cell lysate was used and β-actin was analyzed as loading control. **C,** RNA FISH analysis of STING and cGAS in cells (same as above) treated with 5AZADC same as above. Representative images are shown at ×1,260. Bar size, 400 nm. qPCR analysis of *IFNB* (**D**) and *CXCL10* (**E**) in cells (same as above) treated with 5AZADC followed by dsDNA transfection at 3 μg/mL dsDNA90 for 3 hours. Immunofluorescent microscopy analysis of IRF3 translocation (**F**) and STING translocation (**G**) in indicated cells treated same as in **D**. Representative images are shown at ×1,260. Bar size, 500 nm.

Published OnlineFirst September 28, 2016; DOI: 10.1158/0008-5472.CAN-16-1404

In vivo analysis of melanoma cells response to HSV1γ34.5 therapy

Our *in vitro* analysis indicated that loss of STING signaling may affect the outcome of select oncoviral therapy (Fig. 6A–D). To further evaluate this possibility *in vivo*, we generated melanoma xenografts by subcutaneously inoculating nude mice with melanoma cells harboring partial (RPMI7951 and SK-MEL-3) or defective (A375, MeWo, and SK-MEL-5) STING signaling. HSV1γ34.5 was then administered intratumorally and tumor growth monitored (Fig. 7 and Supplementary Fig. S7). Results showed that tumors derived from melanoma cells with defective STING signaling were extremely susceptible to HSV1γ34.5 treatment (Fig. 7A and B Supplementary Fig. S7). Tumor size decreased rapidly after HSV1γ34.5 treatment. Four of 6 A375 tumors and 3 of 5 SK-MEL-5 tumors diminished 2 to 3 weeks after treatment (Fig. 7A and B). In contrast, tumors derived from melanoma cells exhibiting partial STING signaling (RPMI7951 and SK-MEL-3) were refractory to viral oncolytic treatment (Fig. 7C and D). While these tumors are slow growing *in vivo*, majority of mice did not respond to HSV1γ34.5 therapy at all and the animals were sacked after the tumors burden became significant. Therefore, our findings complement our previous studies and indicate that the ability to measure STING function in melanoma may predict the outcome of DNA virus–related oncolytic therapy against human melanoma and perhaps other type of cancers.

Discussion

STING controls a key innate immune pathway triggered by the presence of cytosolic dsDNA species (7). STING signaling can be triggered by CDN's produced by intracellular bacteria such as *Listeria* monocytogenes (11) or by more recently discovered cGAMP produced by cGAS following association with cytosolic dsDNA species (11, 26). Cytosolic dsDNA can comprise the genome of DNA microbes including DNA viruses such as HSV1 or bacteria such as mycobacterium tuberculosis, as well as self DNA leaked from the nucleus of DNA damaged cells. We have recently demonstrated that STING-deficient mice are susceptible to carcinogen-aggravated CAC (14). DNA damage can trigger STING function intrinsically within the damaged cell, an event that activates production of cytokines that can presumably attract immune cells to the defective cells for phagocytosis before the former can undergo malignant transformation (27–32). Therefore, STING activation may be required to suppress tumorigenesis.

In addition, STING has been reported to be essential for IFNβ-dependent antitumor T-cell responses (33). Data suggest that STING in professional antigen-presenting cells ($CD8^+$ dendritic cells) is activated by the DNA from engulfed dying tumor cells, which results in the production of cytokines, including type I IFN, facilitating cross-presentation and cytotoxic T lymphocyte (CTL) priming (13). Correspondingly, the therapeutic intratumoral administration of CDNs has been shown to repress tumor growth, presumably through activation of STING-facilitated dendritic cell (DC)-dependent CTL production (13, 34). Therefore, both intrinsically and extrinsically activated STING-dependent cytokine production have important roles in suppressing cancer development.

Previously, we have reported that STING signaling is frequently suppressed in human colon cancer. As mentioned, loss of intrinsic STING signal may play a key role in preventing cancer development through inability to respond to DNA damage and alert the immunosurveillance machinery (28, 35). To extend these studies, we analyzed the expression and regulation of STING signaling in melanoma and similarly found that STING-dependent cytokine production was frequently suppressed in human melanoma. Although no significant mutation or deletion events involving the STING or cGAS genes were observed, the inhibition of STING signaling was found to mainly occur through epigenetic suppression of STING and or cGAS expression. Cytosolic DNA–mediated STING signaling was partially rescued by demethylating agent (5AZADC) treatment in some STING-defective melanoma cells, suggesting that DNA hypermethylation is one of the mechanisms for STING/cGAS suppression. However, in other STING-defective melanoma cells, demethylation was not effective in being able to restore STING expression. STING and/or cGAS may selectively become targets for suppression at various stages of cancer development, the suppression of either being sufficient to impede STING function. We have also noticed in some melanoma cells that although both STING/cGAS were expressed, the ability of STING to effectively activate the transcription factors NF-κB or IRF3 was impaired by molecular mechanisms that remain to be determined. Thus, STING function can be impaired at different steps along the signaling pathway, although epigenetic suppression of either STING/cGAS expression seems to be common. Collectively, we observed that STING-dependent signaling was defective in numerous melanomas, which indicated that inhibiting STING function may be a key obligation for the development of melanoma, plausibly enabling such cells to evade the immune system.

Loss of STING may be common in tumors and may even predict outcomes to anticancer therapy. Accordingly, we have developed assays to evaluate the expression levels of both STING and cGAS, loss of either of which will affect STING function. We validated these assays in melanoma and showed that both RNAish-based and IHC-based assays were able to measure STING and cGAS mRNA or protein expression in melanoma cells accurately and sensitively. Using IHC, we screened a melanoma TMA that showed loss of either STING or cGAS in more than 50% malignant and more than 60% metastatic melanomas. Loss of STING function may not be a key tumor onset factor. However, STING does appear to be important in the generation of cytokines in response to DNA damage (14, 15, 30) Loss of STING function is almost certainly important in later stages of cancer development to escape immunosurveillance and host antitumor immunity, especially beneficial in tumor metastasis. Our assays may be useful in predicting the effective response rates of cancers to select therapeutic interventions. Furthermore, recapitulating STING signal in tumors, via novel antitumor gene therapy approaches, may reactivate host antitumor immunity against escaped tumor cells.

Accordingly, we noticed that loss of STING function in melanoma cells rendered cells highly sensitive to DNA virus–mediated oncolytic effect (such as HSV1). Oncolytic HSV1 is one viral therapeutic agent in clinical application. For example, Amgen's talimogene laherparepvec (T-VEC) is an HSV-1–based OV that has been engineered to express GM-CSF to increase immunorecognition. Although T-VEC has shown improved effect over traditional immune therapies for advanced melanoma, the overall response rate is still limited. This phenomenon could be potentially due to diverse STING/cGAS expression status among melanoma cases. OVs may directly destroy the

Published OnlineFirst September 28, 2016; DOI: 10.1158/0008-5472.CAN-16-1404

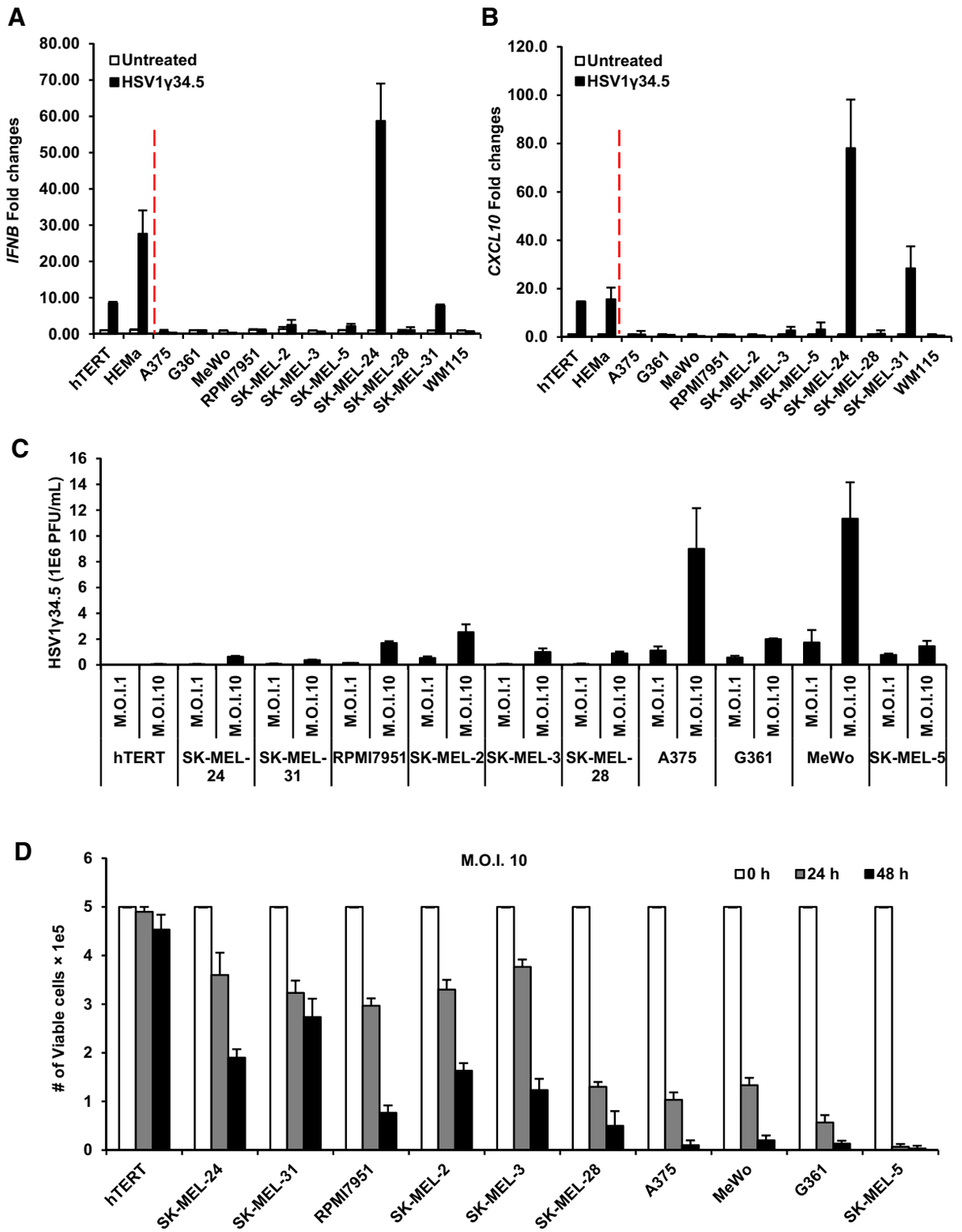

Figure 6.

STING signal defect leads melanoma cells more susceptible to HSV1 infection. Cells (same as in Fig. 1) were infected with HSV1γ34.5 at MOI 5 for 1 hour, and human *IFNB* (**A**) and *CXCL10* (**B**) induction was analyzed by qPCR 3 hours postinfection. **C,** normal hTERT cells and selected human melanoma cell lines were infected with HSV1γ34.5 at MOI 1 or MOI 10 for 1 hour, and titration of HSV1γ34.5 was analyzed by standard plaque assay in vera cells 24 hours later. **D,** cells (same as in **C**) were infected with HSV1γ34.5 at MOI 10 for 1 hour, and cell viability was analyzed by trypan blue staining 24 and 48 hours later.

Published OnlineFirst September 28, 2016; DOI: 10.1158/0008-5472.CAN-16-1404

tumor cell by lysis as well as create a tumor antigen source for activation of antitumor immune response (33). STING may play key roles in both of these processes. Therefore, utilization of STING/cGAS as molecular biomarker may enable a more predictive response to the use of microbes for the treatment of cancer. Such assays may also shed insight into the efficacy of other STING-dependent antitumor therapies based on CDNs or even DNA adduct–based chemotherapeutic regimes (36). Furthermore, gene therapies involving modification of the STING/cGAS status may provide advantages of utilizing host innate and adaptive defense mechanism to facilitate antitumor effects in combination with traditional antitumor therapies. We have noticed that even in the presence of both STING and cGAS, the innate immune signal remains impaired in some melanoma cells, suggesting that other defects in the STING signaling pathway are likely, the causes of which require further elucidation. Thus, further studies on STING signal in cancer development may provide insight into the molecular mechanisms of human carcinogenesis as well as provide novel antitumor therapeutic approaches.

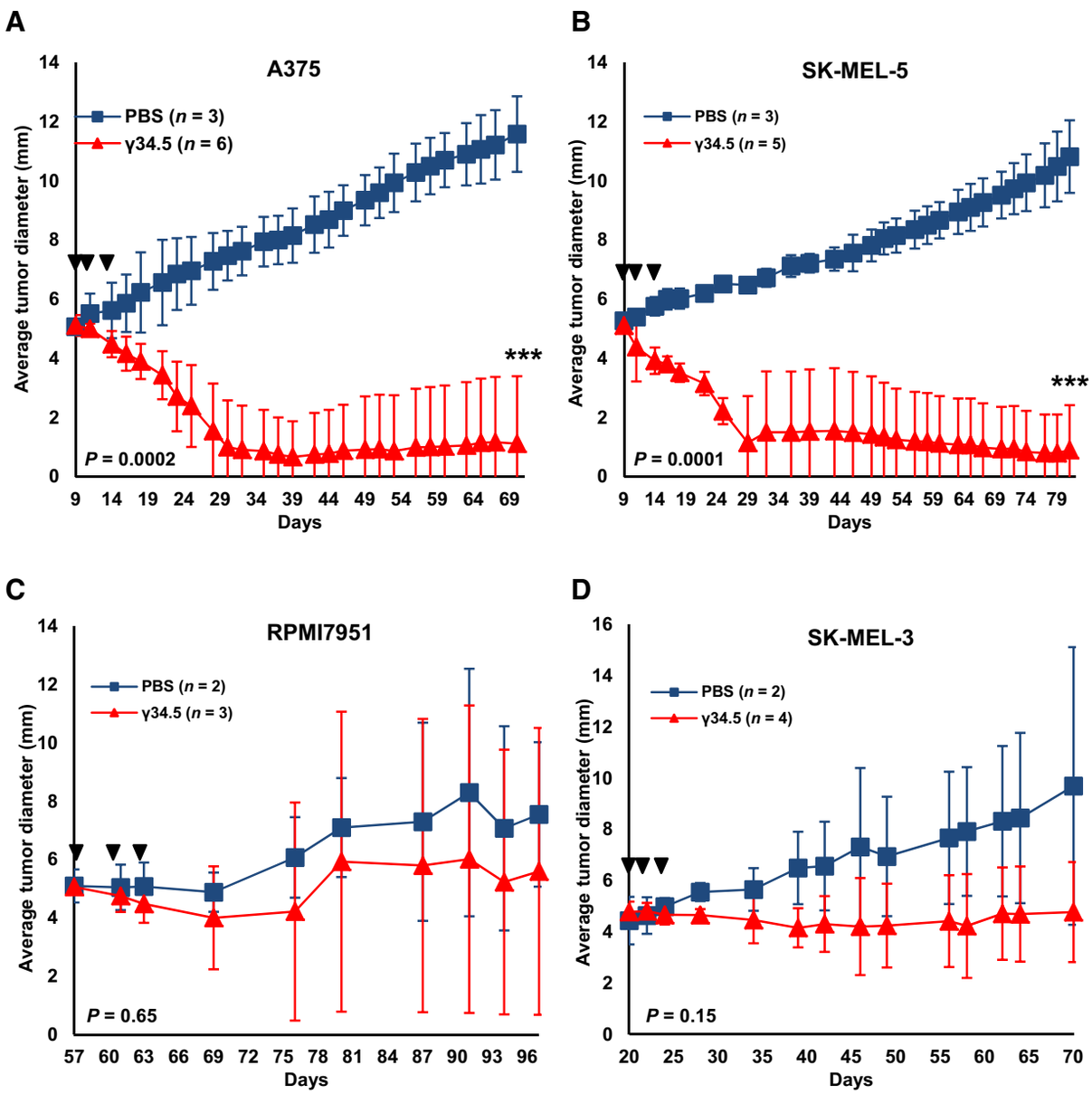

Figure 7.

Increased HSV1γ34.5 oncolytic effect was observed in melanoma xenografts with impaired STING signal *in vivo*. A375 (**A**), SK-MEL-5 (**B**), RPMI7951 (**C**), and SK-MEL-3 (**D**) melanoma xenografts were generated in the right flank of nude Balb/c mice. When tumors had reached approximately 0.5 cm in diameter, tumors were injected every other day a total of three times (arrows) with 1E7 PFU HSV1γ34.5 in 50 μL PBS or 50 μL PBS only and tumor growth measured every other day. Statistical analysis was carried out comparing the two treatment groups at the last time point using the unpaired Student *t* test. *P* values are as indicated.

Disclosure of Potential Conflicts of Interest

No potential conflicts of interest were disclosed.

Authors' Contributions

Conception and design: T. Xia, G.N. Barber
Development of methodology: T. Xia
Acquisition of data (provided animals, acquired and managed patients, provided facilities, etc.): T. Xia, H. Konno
Analysis and interpretation of data (e.g., statistical analysis, biostatistics, computational analysis): T. Xia
Writing, review, and/or revision of the manuscript: T. Xia, G.N. Barber
Study supervision: G.N. Barber

The costs of publication of this article were defrayed in part by the payment of page charges. This article must therefore be hereby marked *advertisement* in accordance with 18 U.S.C. Section 1734 solely to indicate this fact.

Received May 19, 2016; revised August 29, 2016; accepted September 8, 2016; published OnlineFirst September 28, 2016.

References

1. PDQ Adult Treatment Editorial Board. Melanoma treatment (PDQ®): Health Professional Version. In: PDQ Cancer Information Summaries [Internet]. Bethesda, MD: National Cancer Institute; 2002. [cited 2016 Apr 15]. Available from: https://www.ncbi.nlm.nih.gov/books/NBK66034/.
2. Guy GP Jr, Thomas CC, Thompson T, Watson M, Massetti GM, Richardson LC, et al. Vital signs: melanoma incidence and mortality trends and projections - United States, 1982–2030. MMWR Morb Mortal Wkly Rep 2015;64:591–6.
3. Saito Rde F, Tortelli TC Jr, Jacomassi MD, Otake AH, Chammas R. Emerging targets for combination therapy in melanomas. FEBS Lett 2015;589:3438–48.
4. Chin L, Garraway LA, Fisher DE. Malignant melanoma: genetics and therapeutics in the genomic era. Genes Dev 2006;20:2149–82.
5. Andtbacka RH, Kaufman HL, Collichio F, Amatruda T, Senzer N, Chesney J, et al. Talimogene laherparepvec improves durable response rate in patients with advanced melanoma. J Clin Oncol 2015;33:2780–8.
6. Lawler SE, Chiocca EA. Oncolytic virus-mediated immunotherapy: a combinatorial approach for cancer treatment. J Clin Oncol 2015;33:2812–4.
7. Ishikawa H, Barber GN. STING is an endoplasmic reticulum adaptor that facilitates innate immune signalling. Nature 2008;455:674–8.
8. Ahn J, Gutman D, Saijo S, Barber GN. STING manifests self DNA-dependent inflammatory disease. Proc Natl Acad Sci U S A 2012;109:19386–91.
9. Ishikawa H, Ma Z, Barber GN. STING regulates intracellular DNA-mediated, type I interferon-dependent innate immunity. Nature 2009;461:788–92.
10. Sun L, Wu J, Du F, Chen X, Chen ZJ. Cyclic GMP-AMP synthase is a cytosolic DNA sensor that activates the type I interferon pathway. Science 2013;339:786–91.
11. Burdette DL, Monroe KM, Sotelo-Troha K, Iwig JS, Eckert B, Hyodo M, et al. STING is a direct innate immune sensor of cyclic di-GMP. Nature 2011;478:515–8.
12. Hornung V, Hartmann R, Ablasser A, Hopfner KP. OAS proteins and cGAS: unifying concepts in sensing and responding to cytosolic nucleic acids. Nat Rev Immunol 2014;14:521–8.
13. Woo SR, Fuertes MB, Corrales L, Spranger S, Furdyna MJ, Leung MY, et al. STING-dependent cytosolic DNA sensing mediates innate immune recognition of immunogenic tumors. Immunity 2014;41:830–42.
14. Ahn J, Konno H, Barber GN. Diverse roles of STING-dependent signaling on the development of cancer. Oncogene 2015;34:5302–8.
15. Xia T, Konno H, Ahn J, Barber GN. Deregulation of STING signaling in colorectal carcinoma constrains DNA damage responses and correlates with tumorigenesis. Cell Rep 2016;14:282–97.
16. Konno H, Konno K, Barber GN. Cyclic dinucleotides trigger ULK1 (ATG1) phosphorylation of STING to prevent sustained innate immune signaling. Cell 2013;155:688–98.
17. Ahn J, Barber GN. Self-DNA, STING-dependent signaling and the origins of autoinflammatory disease. Curr Opin Immunol 2014;31:121–6.
18. Jin L, Xu LG, Yang IV, Davidson EJ, Schwartz DA, Wurfel MM, et al. Identification and characterization of a loss-of-function human MPYS variant. Genes Immun 2011;12:263–9.
19. Yi G, Brendel VP, Shu C, Li P, Palanathan S, Cheng Kao C. Single nucleotide polymorphisms of human STING can affect innate immune response to cyclic dinucleotides. PLoS One 2013;8:e77846.
20. Lao VV, Grady WM. Epigenetics and colorectal cancer. Nat Rev Gastroenterol Hepatol 2011;8:686–700.
21. Mitchell SM, Ross JP, Drew HR, Ho T, Brown GS, Saunders NF, et al. A panel of genes methylated with high frequency in colorectal cancer. BMC Cancer 2014;14:54.
22. Jin B, Robertson KD. DNA methyltransferases, DNA damage repair, and cancer. Adv Exp Med Biol 2013;754:3–29.
23. Yarbrough ML, Zhang K, Sakthivel R, Forst CV, Posner BA, Barber GN, et al. Primate-specific miR-576–3p sets host defense signalling threshold. Nat Commun 2014;5:4963.
24. Kolodkin-Gal D, Edden Y, Hartshtark Z, Ilan L, Khalaileh A, Pikarsky AJ, et al. Herpes simplex virus delivery to orthotopic rectal carcinoma results in an efficient and selective antitumor effect. Gene Ther 2009;16:905–15.
25. Rowe J, Cen P. TroVax in colorectal cancer. Hum Vaccin Immunother 2014;10:3196–200.
26. Cai X, Chiu YH, Chen ZJ. The cGAS-cGAMP-STING pathway of cytosolic DNA sensing and signaling. Mol Cell 2014;54:289–96.
27. Ahn J, Ruiz P, Barber GN. Intrinsic self-DNA triggers inflammatory disease dependent on STING. J Immunol 2014;193:4634–42.
28. Chatzinikolaou G, Karakasilioti I, Garinis GA. DNA damage and innate immunity: links and trade-offs. Trends Immunol 2014;35:429–35.
29. Kidane D, Chae WJ, Czochor J, Eckert KA, Glazer PM, Bothwell AL, et al. Interplay between DNA repair and inflammation, and the link to cancer. Crit Rev Biochem Mol Biol 2014;49:116–39.
30. Ahn J, Xia T, Konno H, Konno K, Ruiz P, Barber GN. Inflammation-driven carcinogenesis is mediated through STING. Nat Commun 2014;5:5166.
31. Deng L, Liang H, Xu M, Yang X, Burnette B, Arina A, et al. STING-dependent cytosolic DNA sensing promotes radiation-induced type I interferon-dependent antitumor immunity in immunogenic tumors. Immunity 2014;41:843–52.
32. Zhu Q, Man SM, Gurung P, Liu Z, Vogel P, Lamkanfi M, et al. Cutting edge: STING mediates protection against colorectal tumorigenesis by governing the magnitude of intestinal inflammation. J Immunol 2014;193:4779–82.
33. Woo SR, Corrales L, Gajewski TF. The STING pathway and the T cell-inflamed tumor microenvironment. Trends Immunol 2015;36:250–6.
34. Corrales L, Glickman LH, McWhirter SM, Kanne DB, Sivick KE, Katibah GE, et al. Direct activation of STING in the tumor microenvironment leads to potent and systemic tumor regression and immunity. Cell Rep 2015;11:1018–30.
35. Kondo T, Kobayashi J, Saitoh T, Maruyama K, Ishii KJ, Barber GN, et al. DNA damage sensor MRE11 recognizes cytosolic double-stranded DNA and induces type I interferon by regulating STING trafficking. Proc Natl Acad Sci U S A 2013;110:2969–74.
36. Zitvogel L, Galluzzi L, Smyth MJ, Kroemer G. Mechanism of action of conventional and targeted anticancer therapies: reinstating immunosurveillance. Immunity 2013;39:74–88.

Published OnlineFirst September 28, 2016; DOI: 10.1158/0008-5472.CAN-16-1404

Cancer Research
The Journal of Cancer Research (1916–1930) | The American Journal of Cancer (1931–1940)

AACR American Association for Cancer Research

Recurrent Loss of STING Signaling in Melanoma Correlates with Susceptibility to Viral Oncolysis

Tianli Xia, Hiroyasu Konno and Glen N. Barber

Cancer Res 2016;76:6747-6759. Published OnlineFirst September 28, 2016.

Cancer Research
Supplementary Data Summary

Recurrent loss of STING Signaling in Melanoma Correlates with Susceptibility to Viral Oncolysis.

Tianli Xia, Hiroyasu Konno and Glen N. Barber

I. Supplementary Figures

1. Figure S1, dsDNA90 Transfection efficiency in melanoma cells.
2. Figure S2, si-STING effect on melanoma cells.
3. Figure S3, Cisplatin treatment in melanoma cells and cGAS immuoblot verification.
4. Figure S4, additional immunofluorescence analysis in melanoma cells.
5. Figure S5, schematic diagram of predicted CpG islands in STING promoter.
6. Figure S6, vaccinia virus treatment in melanoma cells.
7. Figure S7, HSV1γ34.5 treatment on MeWo xenograft in vivo.

II. Supplementary Tables

1. Table S1, IHC analysis of STING and cGAS in Melanoma Tissue Microarray.
2. Table S2, sequencing of STING in Melanoma Cell Lines.
3. Table S3, sequencing of cGAS in Melanoma Cell Lines.

Supplementary Figure S1.

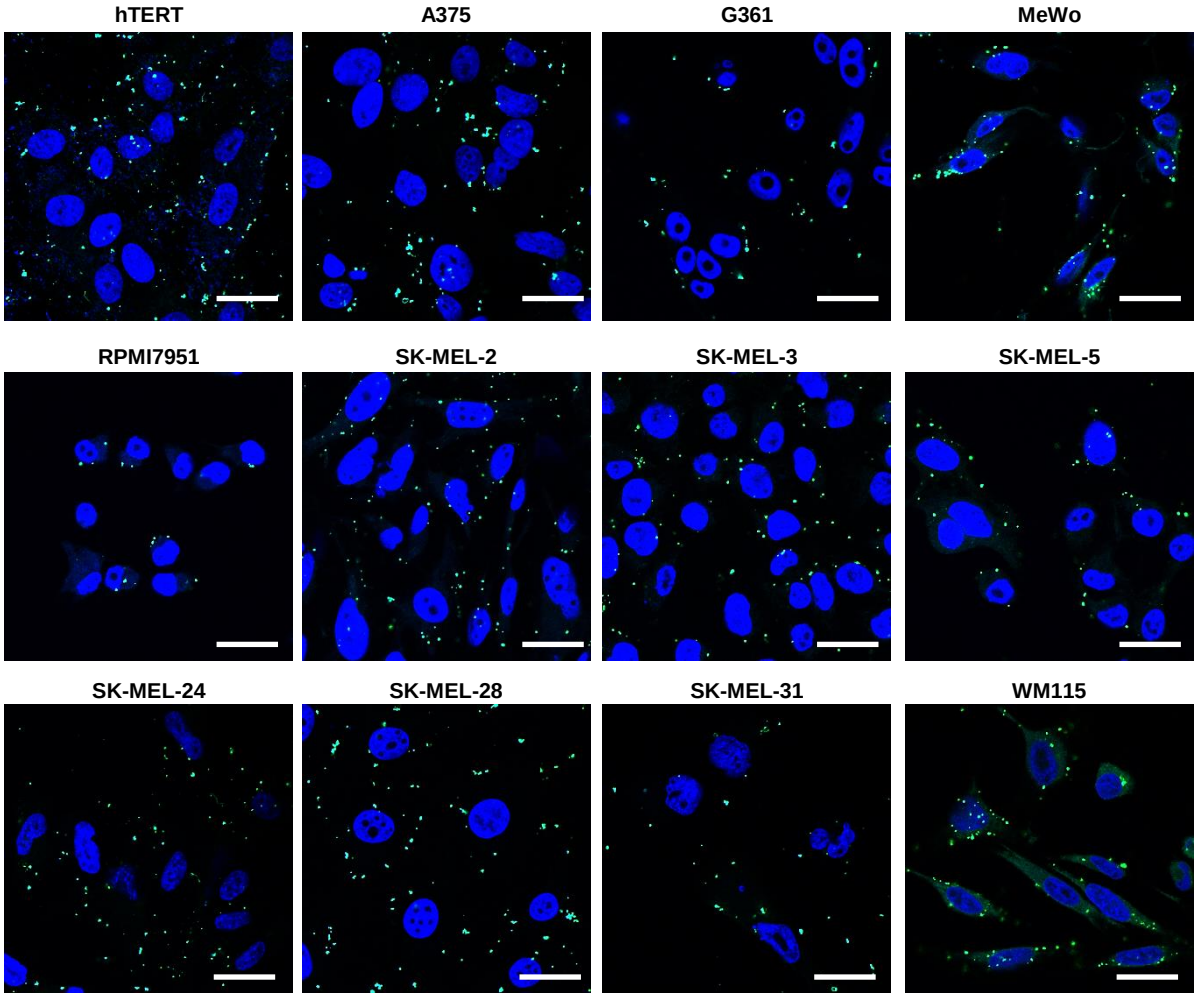

Supplementary Figure S1. dsDNA90 Transfection efficiency into Melanoma Cell Lines were monitor with FITC-dsDNA90 3 hours post Lipofectamine 2000 transfection under fluorescent microscopy. Images shown are at 600X. Bar size, 5µm.

Supplementary Figure S2.

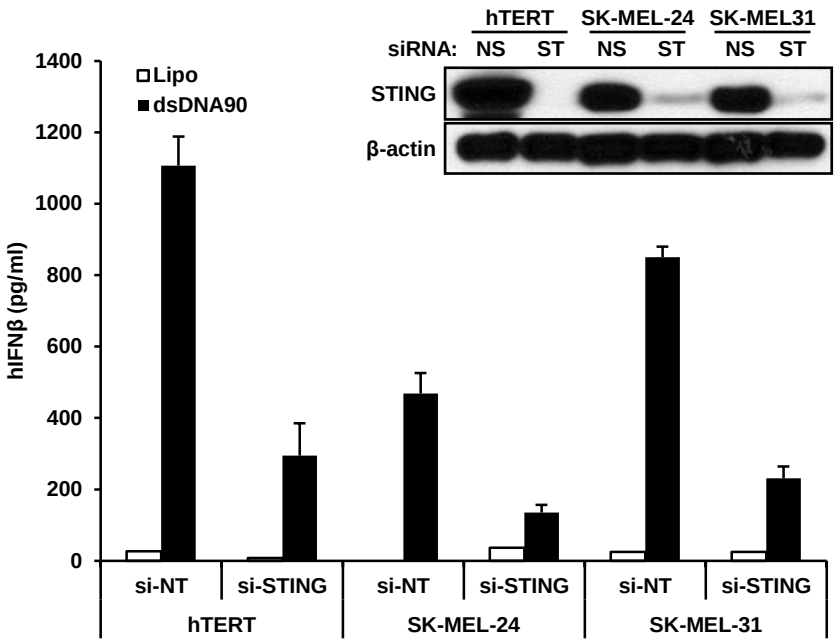

Supplementary Figure S2. Normal hTERT and Melanoma cells were treated with non-specific siRNA (si-NT) or STING siRNA (si-STING) for 3 days followed by dsDNA90 transfection at 3µg/ml for 16 hours. Culture supernatant were then analyzed for hFNβ by Elisa and cell lysates were analyzed for STING siRNA efficiency by immunoblot (inlet).

Supplementary Figure S3.

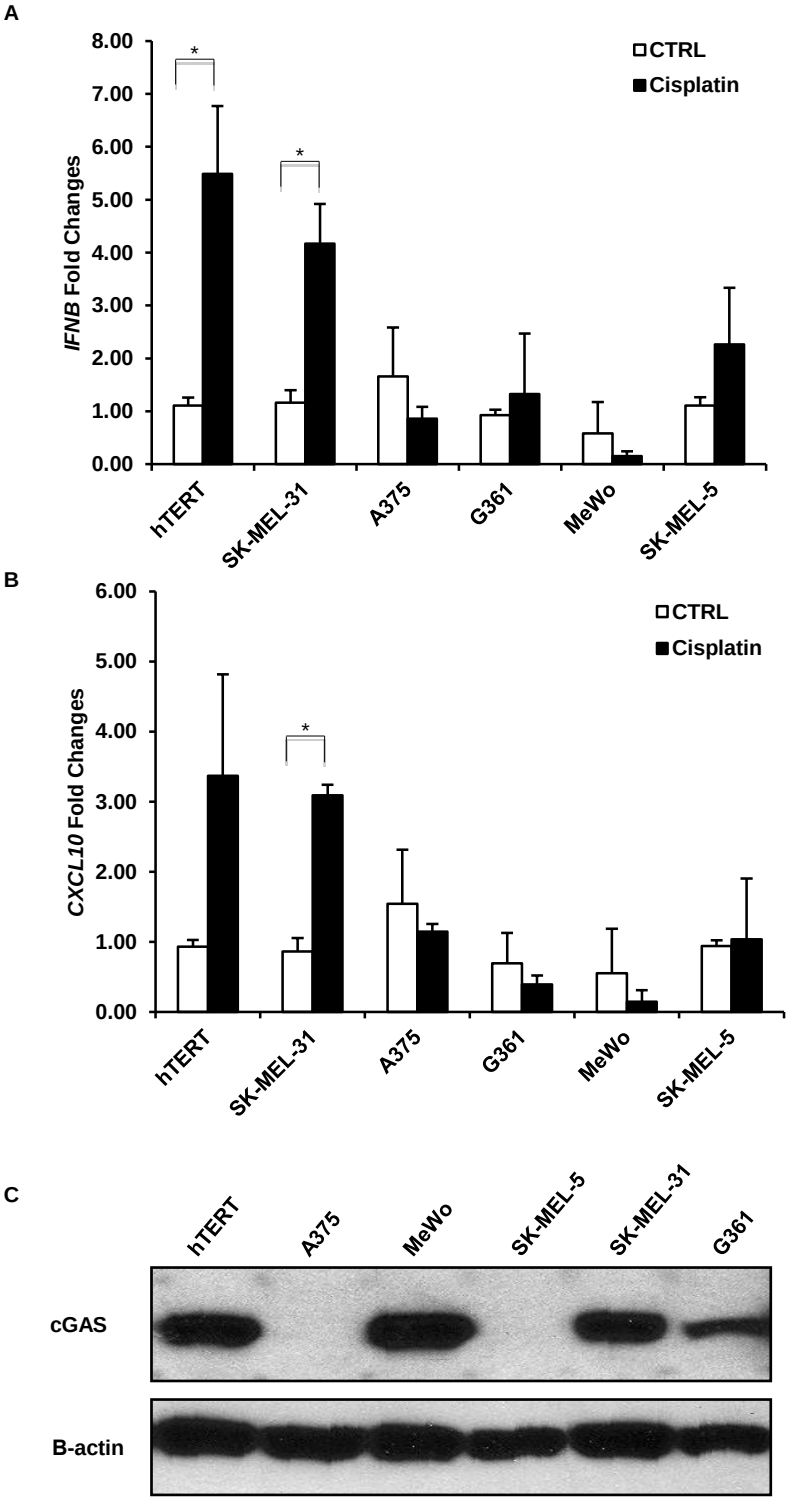

Supplementary Figure S3. Normal hTERT and Melanoma cells were treated with 10 µM of Cisplatin for 48 hours and analyzed by qPCR for (**A**) *IFNB* and (**B**) *CXCL10* induction. **C**. Immunoblot analysis of cGAS in normal and melanoma cell lines. 50 µg whole cell lysate was used. B-actin was analyzed as loading control.

Supplementary Figure S4.

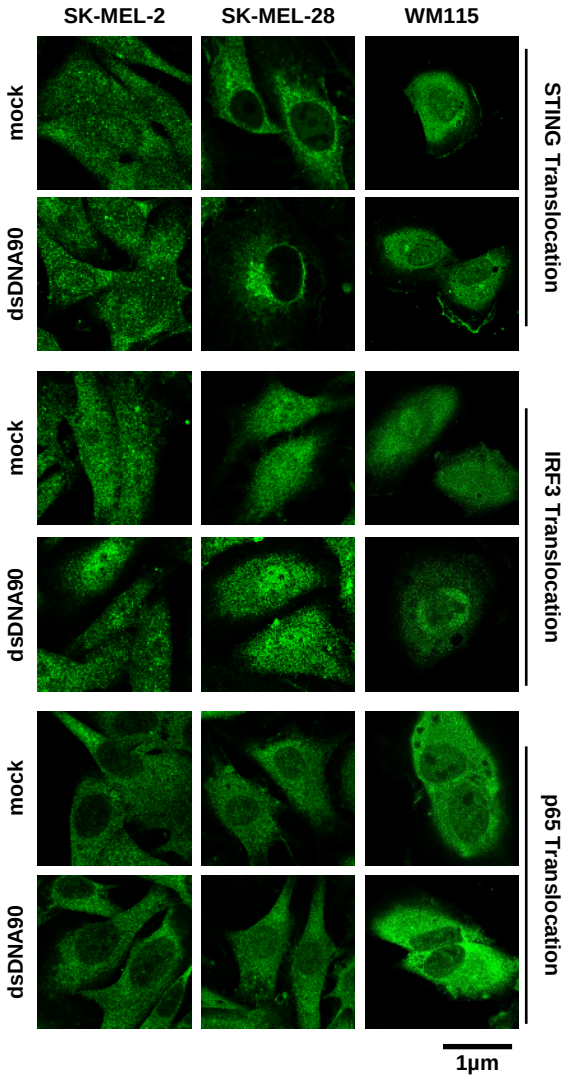

Supplementary Figure S4. Immunofluorescence Microscopy analysis of STING, IRF3 and p65 translocation in human melanoma cell lines transfected with 3µg/ml dsDNA90 or mock transfected for 3 hours. Original magnification, 1260X. Bar size, 1µm.

Supplementary Figure S5.

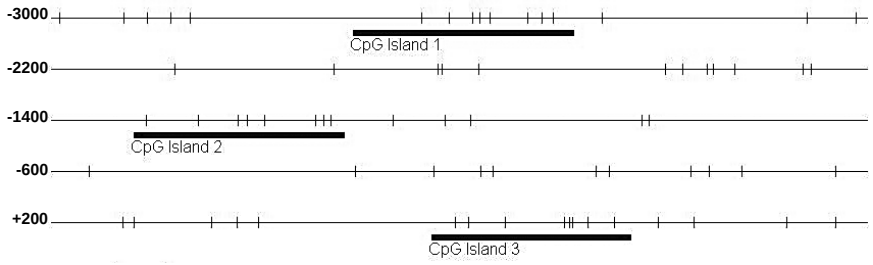

CGI1: %GC=50.0, Obs/Exp=0.610, Length=218
CGI2: %GC=50.5, Obs/Exp=0.608, Length=208
CGI3: %GC=51.8, Obs/Exp=0.606, Length=197

Supplementary Figure S5. Schematic representation of CpG Islands located in the proximal promoter regions of STING.

Supplementary Figure S6.

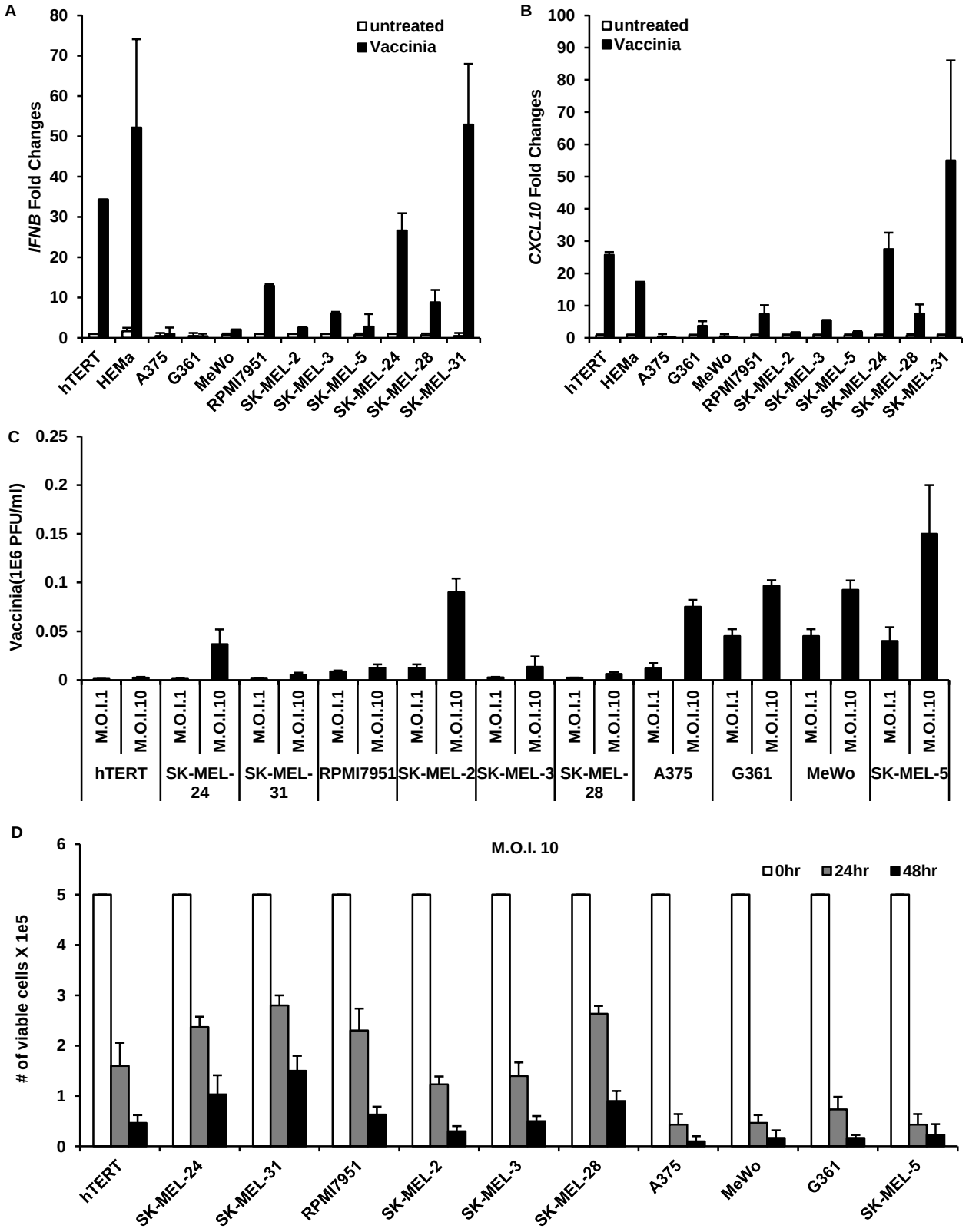

Supplementary Figure S6. STING signal defect leads melanoma cells more susceptible to Vaccinia Virus infection. Normal and Melanoma Cells were infected with Vaccinia Virus at M.O.I. 10 for 1 hour and human *IFNB* (**A**) and *CXCL10* (**B**) induction was analyzed by qPCR 3 hours post infection. **C**, Cells were infected with Vaccinia Virus at M.O.I. 1 or M.O.I. 10 for 1 hour, and virus titration was analyzed by standard plaque assay in Vero cells 24 hours post infection. **D**, Cells were infected with Vaccinia Virus at M.O.I. 10 for 1 hour, and cell viability was analyzed by trypan blue staining 24 hours and 48 hours post infection.

Supplementary Figure S7.

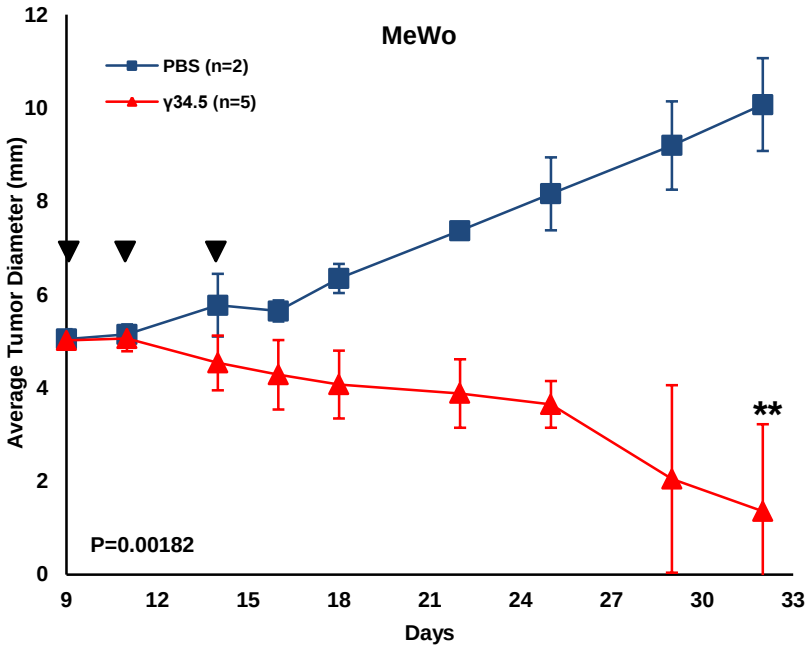

Supplementary Figure S7. MeWo melanoma xenografts were generated in the right flank of nude Balb/c mice. When tumors had reached approximately 0.5 cm in diameter, tumors were injected every other day a total of three times (arrows) with 1E7 PFU HSV1γ34.5 in 50 µl PBS or 50 µl PBS only and tumor growth measured every other day. Statistical analysis was carried out comparing the two treatment groups at the last time point using the unpaired Student's t-test. P values are as indicated; **, P<0.01.

Supplementary Table S1. IHC analysis of STING and cGAS in Human Melanoma Tissue Microarray I.

Type	Position	Sex	Age	Pathology	STING				cGAS			
					Area	Intensity	H-Score	Status	Area	Intensity	H-Score	Status
Normal	A01	M	37	Normal	3	3	9	+	2	2	4	+
	A02	M	43	Normal	3	3	9	+	3	3	9	+
	A03	F	33	Normal	3	3	9	+	3	2	6	+
	A04	F	47	Normal	3	3	9	+	3	2	6	+
	B01	M	37	Normal	3	3	9	+	3	2	6	+
	B02	M	43	Normal	3	3	9	+	3	3	9	+
	B03	F	33	Normal	3	3	9	+	3	2	6	+
	B04	F	47	Normal	3	3	9	+	3	2	6	+
Benign	A05	F	15	Intraepidermal nevus	3	3	9	+	0	0	0	-
	A06	F	19	Compound nevus	3	3	9	+	3	1	3	+
	A07	F	37	Compund nevus	3	3	9	+	3	1	3	+
	A08	F	27	Intraepidermal nevus	3	3	9	+	2	3	6	+
	B05	F	15	Intraepidermal nevus	3	3	9	+	0	0	0	-
	B06	F	19	Compound nevus	3	3	9	+	2	3	6	+
	B07	F	37	Compund nevus	3	3	9	+	3	2	6	+
	B08	F	27	Intraepidermal nevus	3	2	6	+	3	2	6	+
Malignant	A09	M	69	Basal cell carcinoma	3	3	9	+	1	2	2	-
	A10	M	38	Basal cell carcinoma	3	2	6	+	0	0	0	-
	A11	M	67	Squamous cell carcinoma	3	1	3	-	2	1	2	-
	A12	M	34	Squamous cell carcinoma	0	0	0	-	3	1	3	+
	B09	M	69	Basal cell carcinoma	3	3	9	+	3	2	6	+
	B10	M	38	Basal cell carcinoma	3	3	9	+	1	3	3	+
	B11	M	67	Squamous cell carcinoma	2	1	2	-	1	2	2	-
	B12	M	34	Squamous cell carcinoma	0	0	0	-	3	1	3	+
	C01	F	23	Melanoma	2	3	6	+	3	1	3	+
	C02	M	11	Melanoma	3	3	9	+	2	2	4	+
	C03	F	77	Melanoma	3	2	6	+	3	2	6	+
	C04	M	84	Melanoma	3	3	9	+	3	3	9	+
	C05	M	25	Melanoma	3	2	6	+	2	1	2	-
	C06	F	45	Melanoma	3	1	3	-	1	1	1	-
	C07	F	53	Melanoma	3	2	6	+	2	3	6	+
	C08	M	53	Melanoma	3	3	9	+	1	3	3	+
	C09	M	29	Melanoma	3	1	3	-	3	1	3	+
	C10	M	74	Melanoma	0	0	0	-	0	0	0	-
	C11	F	53	Melanoma	2	1	2	-	3	1	3	+
	C12	F	80	Melanoma	3	3	9	+	3	3	9	+
	D01	F	23	Melanoma	3	2	6	+	3	1	3	+
	D02	M	11	Melanoma	3	1	3	-	3	2	6	+
	D03	F	77	Melanoma	3	3	9	+	2	2	4	+
	D04	M	84	Melanoma	3	3	9	+	3	3	9	+
	D05	M	25	Melanoma	0	0	0	-	0	0	0	-
	D06	F	45	Melanoma	1	2	2	-	3	1	3	+
	D07	F	53	Melanoma	2	3	6	+	2	2	4	+
	D08	M	53	Melanoma	0	0	0	-	2	1	2	-
	D09	M	29	Melanoma	0	0	0	-	3	1	3	+
	D10	M	74	Melanoma	0	0	0	-	3	1	3	+
	D11	F	53	Melanoma	2	3	6	+	1	3	3	+
	D12	F	80	Melanoma	3	3	9	+	3	3	9	+
	E01	M	64	Melanoma	3	3	9	+	2	1	2	-
	E02	M	25	Melanoma	3	3	9	+	2	1	2	-
	E03	F	56	Melanoma	3	2	6	+	3	1	3	+
	E04	M	64	Melanoma	3	3	9	+	2	1	2	-
	E05	F	72	Melanoma	2	2	4	+	3	1	3	+
	E06	F	54	Melanoma	0	0	0	-	2	2	4	+

	E07	F	63	Melanoma	3	1	3	-	3	2	6	+
	E08	F	57	Melanoma	0	0	0	-	3	1	3	+
	E09	M	59	Melanoma	3	3	9	+	3	3	9	+
	E10	F	56	Melanoma	2	3	6	+	3	3	9	+
	E11	F	60	Melanoma	2	3	6	+	2	3	6	+
	E12	F	48	Melanoma	3	3	9	+	3	3	9	+
	F01	M	64	Melanoma	3	2	6	+	2	1	2	-
	F02	M	25	Melanoma	3	3	9	+	1	2	2	-
	F03	F	56	Melanoma	3	2	6	+	3	1	3	+
	F04	M	64	Melanoma	3	3	9	+	0	0	0	-
	F05	F	72	Melanoma	1	3	3	-	2	2	4	+
	F06	F	54	Melanoma	1	3	3	-	3	1	3	+
	F07	F	63	Melanoma	1	2	2	-	2	1	2	-
	F08	F	57	Melanoma	0	0	0	-	0	0	0	-
	F09	M	59	Melanoma	3	3	9	+	3	3	9	+
	F10	F	56	Melanoma	3	3	9	+	3	3	9	+
	F11	F	60	Melanoma	3	3	9	+	3	3	9	+
	F12	F	48	Melanoma	3	3	9	+	2	3	6	+
Metastatic	G01	M	25	Metastatic melanoma	3	1	3	-	0	0	0	-
	G02	M	57	Metastatic melanoma	3	3	9	+	3	3	9	+
	G03	F	53	Metastatic melanoma	3	2	6	+	2	1	2	-
	G04	F	48	Metastatic melanoma	3	3	9	+	3	3	9	+
	G05	M	44	Metastatic melanoma	3	3	9	+	3	3	9	+
	G06	M	45	Metastatic melanoma	3	1	3	-	0	0	0	-
	G07	F	71	Metastatic melanoma	3	3	9	+	3	3	9	+
	G08	M	69	Metastatic melanoma	1	3	3	-	2	3	6	+
	G09	M	44	Metastatic melanoma	3	1	3	-	0	0	0	-
	G10	M	48	Metastatic melanoma	0	0	0	-	2	1	2	-
	G11	M	73	Metastatic melanoma	0	0	0	-	2	1	2	-
	G12	M	57	Metastatic melanoma	3	1	3	-	2	1	2	-
	H01	M	25	Metastatic melanoma	3	2	6	+	2	1	2	-
	H02	M	57	Metastatic melanoma	3	3	9	+	2	3	6	+
	H03	F	53	Metastatic melanoma	3	2	6	+	0	0	0	-
	H04	F	48	Metastatic melanoma	3	3	9	+	1	3	3	+
	H05	M	44	Metastatic melanoma	3	3	9	+	3	3	9	+
	H06	M	45	Metastatic melanoma	0	0	0	-	0	0	0	-
	H07	F	71	Metastatic melanoma	3	3	9	+	3	3	9	+
	H08	M	69	Metastatic melanoma	0	0	0	-	1	2	2	-
	H09	M	44	Metastatic melanoma	3	1	3	-	1	1	1	-
	H10	M	48	Metastatic melanoma	1	3	3	-	2	3	6	+
	H11	M	73	Metastatic melanoma	3	1	3	-	2	1	2	-
	H12	M	57	Metastatic melanoma	2	3	6	+	3	1	3	+

II.

Type	STING expression		cGAS expression	
	H-Score	p-Value	H-Score	p-Value
Normal	9±0 (n=8)	N/A	6.5±1.7 (n=8)	N/A
Benign	8.6±1.1 (n=8)	0.167	3.8±2.7 (n=8)	0.013*
Malignant	5.4±3.5 (n=56)	0.002**	4±2.8 (n=56)	0.009**
Metastatic	5±3.4 (n=24)	0.001**	3.9±3.5 (n=24)	0.026*

Supplementary Table S2. Sequencing *STING* in Human Melanoma Cell Lines

Sample Name	Age	Gender	Ethnicity	Pathology	Target Region	Position in Target	Ref. Base	Variant Found	Variant Name	Variant Class	Variant Function	Reference Codon	Variant Codon
HEMa	normal human epidermal melanocytes				TMEM173_Exon3	144	G	C	rs7447927	SNP	Coding, Synon.	GTG=Val	GTC=Val
					TMEM173_Exon6	175	A	G	rs1131769	SNP	Coding, Non-Synon.	CAT=His	CGT=Arg
					TMEM173_Intron5_3	144	C	Y	rs116583357	SNP	Intronic		
A375	54	female		malignant melanoma	TMEM173_Exon3	144	G	C	rs7447927	SNP	Coding, Synon.	GTG=Val	GTC=Val
					TMEM173_Exon6	175	A	G	rs1131769	SNP	Coding, Non-Synon.	CAT=His	CGT=Arg
G361	31	male	Caucasian	malignant melanoma	TMEM173_Exon3	144	G	C	rs7447927	SNP	Coding, Synon.	GTG=Val	GTC=Val
					TMEM173_Exon6	175	A	G	rs1131769	SNP	Coding, Non-Synon.	CAT=His	CGT=Arg
MeWo	78	male	Caucasian	malignant melanoma	TMEM173_Exon3	212	G	R	rs11554776	SNP	Coding, Non-Synon.	CGC=Arg	CAC=His
					TMEM173_Exon6	169	G	S	rs78233829	SNP	Coding, Non-Synon.	GGT=Gly	GCT=Ala
					TMEM173_Exon6	175	A	R	rs1131769	SNP	Coding, Non-Synon.	CAT=His	CGT=Arg
					TMEM173_Exon7	119	G	R	rs7380824	SNP	Coding, Non-Synon.	CGG=Arg	CAG=Gln
					TMEM173_Intron4	140	G	R	rs7380272	SNP	Intronic		
					TMEM173_Intron4	215	G	R	rs148884539	SNP	Intronic		
					TMEM173_Intron6_3	3	A	R	rs75746446	SNP	Intronic		
					TMEM173_Intron7_2	52	G	S	rs73257329	SNP	Intronic		
					TMEM173_Intron7_3	79	C	Y	Novel	SNP	Intronic		
RPMI7951	18	female	Caucasian	malignant melanoma	TMEM173_Exon3	144	G	C	rs7447927	SNP	Coding, Synon.	GTG=Val	GTC=Val
					TMEM173_Exon6	175	A	G	rs1131769	SNP	Coding, Non-Synon.	CAT=His	CGT=Arg
SK-MEL-2	60	male	Caucasian	malignant melanoma	TMEM173_Exon3	144	G	S	rs7447927	SNP	Coding, Synon.	GTG=Val	GTC=Val
					TMEM173_Exon3	212	G	R	rs11554776	SNP	Coding, Non-Synon.	CGC=Arg	CAC=His
					TMEM173_Exon6	169	G	S	rs78233829	SNP	Coding, Non-Synon.	GGT=Gly	GCT=Ala
					TMEM173_Exon6	175	A	G	rs1131769	SNP	Coding, Non-Synon.	CAT=His	CGT=Arg
					TMEM173_Exon7	119	G	R	rs7380824	SNP	Coding, Non-Synon.	CGG=Arg	CAG=Gln
					TMEM173_Intron4	140	G	R	rs7380272	SNP	Intronic		
					TMEM173_Intron6_3	3	A	R	rs75746446	SNP	Intronic		
					TMEM173_Intron7_2	52	G	S	rs73257329	SNP	Intronic		
SK-MEL-3	42	female	Caucasian	malignant melanoma	TMEM173_Exon3	212	G	R	rs11554776	SNP	Coding, Non-Synon.	CGC=Arg	CAC=His
					TMEM173_Exon6	169	G	S	rs78233829	SNP	Coding, Non-Synon.	GGT=Gly	GCT=Ala
					TMEM173_Exon6	175	A	G	rs1131769	SNP	Coding, Non-Synon.	CAT=His	CGT=Arg
					TMEM173_Exon7	119	G	R	rs7380824	SNP	Coding, Non-Synon.	CGG=Arg	CAG=Gln
					TMEM173_Intron4	140	G	R	rs7380272	SNP	Intronic		
					TMEM173_Intron6_3	3	A	R	rs75746446	SNP	Intronic		
SK-MEL-5	24	female	Caucasian	malignant melanoma	TMEM173_Exon3	144	G	S	rs7447927	SNP	Coding, Synon.	GTG=Val	GTC=Val
					TMEM173_Exon6	175	A	R	rs1131769	SNP	Coding, Non-Synon.	CAT=His	CGT=Arg
SK-MEL-24	67	male	Caucasian	malignant melanoma	TMEM173_Exon3	144	G	S	rs7447927	SNP	Coding, Synon.	GTG=Val	GTC=Val
					TMEM173_Exon3	212	G	R	rs11554776	SNP	Coding, Non-Synon.	CGC=Arg	CAC=His
					TMEM173_Exon6	169	G	S	rs78233829	SNP	Coding, Non-Synon.	GGT=Gly	GCT=Ala
					TMEM173_Exon6	175	A	G	rs1131769	SNP	Coding, Non-Synon.	CAT=His	CGT=Arg
					TMEM173_Exon7	119	G	R	rs7380824	SNP	Coding, Non-Synon.	CGG=Arg	CAG=Gln
					TMEM173_Intron4	140	G	R	rs7380272	SNP	Intronic		
					TMEM173_Intron6_3	3	A	R	rs75746446	SNP	Intronic		
SK-MEL-28	51	male		malignant melanoma	TMEM173_Exon3	212	G	A	rs11554776	SNP	Coding, Non-Synon.	CGC=Arg	CAC=His
					TMEM173_Exon6	169	G	C	rs78233829	SNP	Coding, Non-Synon.	GGT=Gly	GCT=Ala
					TMEM173_Exon6	175	A	G	rs1131769	SNP	Coding, Non-Synon.	CAT=His	CGT=Arg
					TMEM173_Exon7	119	G	A	rs7380824	SNP	Coding, Non-Synon.	CGG=Arg	CAG=Gln
					TMEM173_Intron4	140	G	A	rs7380272	SNP	Intronic		
					TMEM173_Intron6_3	3	A	G	rs75746446	SNP	Intronic		
					TMEM173_Intron7_2	52	G	C	rs73257329	SNP	Intronic		
SK-MEL-31		female		malignant melanoma	TMEM173_Exon3	144	G	S	rs7447927	SNP	Coding, Synon.	GTG=Val	GTC=Val
					TMEM173_Exon3	212	G	R	rs11554776	SNP	Coding, Non-Synon.	CGC=Arg	CAC=His
					TMEM173_Exon6	169	G	S	rs78233829	SNP	Coding, Non-Synon.	GGT=Gly	GCT=Ala
					TMEM173_Exon6	175	A	G	rs1131769	SNP	Coding, Non-Synon.	CAT=His	CGT=Arg
					TMEM173_Exon7	119	G	R	rs7380824	SNP	Coding, Non-Synon.	CGG=Arg	CAG=Gln
					TMEM173_Intron4	140	G	R	rs7380272	SNP	Intronic		
					TMEM173_Intron6_3	3	A	R	rs75746446	SNP	Intronic		
					TMEM173_Intron7_2	52	G	S	rs73257329	SNP	Intronic		
WM115	58	female		melanoma	TMEM173_Exon3	212	G	A	rs11554776	SNP	Coding, Non-Synon.	CGC=Arg	CAC=His
					TMEM173_Exon6	169	G	C	rs78233829	SNP	Coding, Non-Synon.	GGT=Gly	GCT=Ala
					TMEM173_Exon6	175	A	G	rs1131769	SNP	Coding, Non-Synon.	CAT=His	CGT=Arg
					TMEM173_Exon7	119	G	A	rs7380824	SNP	Coding, Non-Synon.	CGG=Arg	CAG=Gln
					TMEM173_Intron4	140	G	A	rs7380272	SNP	Intronic		
					TMEM173_Intron6_3	3	A	G	rs75746446	SNP	Intronic		

Supplementary Table S3. Sequencing *cGAS* in Human Melanoma Cell Lines

Sample Name	Age	Gender	Ethnicity	Pathology	Target Region	Position in Target	Ref. Base	Variant Found	Variant Name	Variant Class	Variant Function	Reference Codon	Variant Codon
HEMa	normal human epidermal melanocytes				MB21D1_Exon1_1	243	C	A	rs9352000	SNP	Coding, Non-Synon.	ACC=Thr	AAC=Asn
					MB21D1_Exon1_2	11	C	M	rs35629782	SNP	Coding, Non-Synon.	GCG=Ala	GAG=Glu
					MB21D1_Exon1_3	11	T	C	rs9446904	SNP	Coding, Synon.	CCT=Pro	CCC=Pro
					MB21D1_Exon2	125	C	A	rs610913	SNP	Coding, Non-Synon.	CCT=Pro	CAT=His
					MB21D1_Exon5_2	70	G	R	rs311678	SNP	Coding, Synon.	AAG=Lys	AAA=Lys
A375	54	female		malignant melanoma	MB21D1_Exon1_1	33	T	HD	rs34413328	Deletion	UTR		
					MB21D1_Exon1_1	243	C	A	rs9352000	SNP	Coding, Non-Synon.	ACC=Thr	AAC=Asn
					MB21D1_Exon1_3	11	T	C	rs9446904	SNP	Coding, Synon.	CCT=Pro	CCC=Pro
					MB21D1_Exon5_2	70	G	R	rs311678	SNP	Coding, Synon.	AAG=Lys	AAA=Lys
G361	31	male	Caucasian	malignant melanoma									
MeWo	78	male	Caucasian	malignant melanoma	MB21D1_Exon1_1	243	C	M	rs9352000	SNP	Coding, Non-Synon.	ACC=Thr	AAC=Asn
					MB21D1_Exon1_3	11	T	Y	rs9446904	SNP	Coding, Synon.	CCT=Pro	CCC=Pro
					MB21D1_Exon5_2	70	G	A	rs311678	SNP	Coding, Synon.	AAG=Lys	AAA=Lys
RPMI7951	18	female	Caucasian	malignant melanoma	MB21D1_Exon1_1	33	T	HD	rs34413328	Deletion	UTR		
					MB21D1_Exon1_1	243	C	A	rs9352000	SNP	Coding, Non-Synon.	ACC=Thr	AAC=Asn
					MB21D1_Exon1_2	11	C	M	rs35629782	SNP	Coding, Non-Synon.	GCG=Ala	GAG=Glu
					MB21D1_Exon1_3	11	T	C	rs9446904	SNP	Coding, Synon.	CCT=Pro	CCC=Pro
					MB21D1_Exon5_2	70	G	R	rs311678	SNP	Coding, Synon.	AAG=Lys	AAA=Lys
SK-MEL-2	60	male	Caucasian	malignant melanoma	MB21D1_Exon1_1	243	C	M	rs9352000	SNP	Coding, Non-Synon.	ACC=Thr	AAC=Asn
					MB21D1_Exon1_3	11	T	Y	rs9446904	SNP	Coding, Synon.	CCT=Pro	CCC=Pro
					MB21D1_Exon5_2	70	G	R	rs311678	SNP	Coding, Synon.	AAG=Lys	AAA=Lys
SK-MEL-3	42	female	Caucasian	malignant melanoma	MB21D1_Exon1_1	33	T	-	rs34413328	Deletion	UTR		
					MB21D1_Exon1_1	243	C	A	rs9352000	SNP	Coding, Non-Synon.	ACC=Thr	AAC=Asn
					MB21D1_Exon1_3	11	T	C	rs9446904	SNP	Coding, Synon.	CCT=Pro	CCC=Pro
					MB21D1_Exon5_2	70	G	R	rs311678	SNP	Coding, Synon.	AAG=Lys	AAA=Lys
SK-MEL-5	24	female	Caucasian	malignant melanoma	MB21D1_Exon1_1	33	T	-	rs34413328	Deletion	UTR		
					MB21D1_Exon1_1	243	C	A	rs9352000	SNP	Coding, Non-Synon.	ACC=Thr	AAC=Asn
					MB21D1_Exon1_3	11	T	C	rs9446904	SNP	Coding, Synon.	CCT=Pro	CCC=Pro
SK-MEL-24	67	male	Caucasian	malignant melanoma	MB21D1_Exon1_1	243	C	M	rs9352000	SNP	Coding, Non-Synon.	ACC=Thr	AAC=Asn
					MB21D1_Exon1_3	11	T	Y	rs9446904	SNP	Coding, Synon.	CCT=Pro	CCC=Pro
					MB21D1_Exon2	125	C	M	rs610913	SNP	Coding, Non-Synon.	CCT=Pro	CAT=His
					MB21D1_Exon5_2	70	G	R	rs311678	SNP	Coding, Synon.	AAG=Lys	AAA=Lys
SK-MEL-28	51	male		malignant melanoma	MB21D1_Exon1_1	243	C	A	rs9352000	SNP	Coding, Non-Synon.	ACC=Thr	AAC=Asn
					MB21D1_Exon1_3	11	T	C	rs9446904	SNP	Coding, Synon.	CCT=Pro	CCC=Pro
					MB21D1_Exon5_2	70	G	A	rs311678	SNP	Coding, Synon.	AAG=Lys	AAA=Lys
SK-MEL-31		female		malignant melanoma	MB21D1_Exon1_1	33	T	-	rs34413328	Deletion	UTR		
					MB21D1_Exon1_1	243	C	A	rs9352000	SNP	Coding, Non-Synon.	ACC=Thr	AAC=Asn
					MB21D1_Exon1_3	11	T	C	rs9446904	SNP	Coding, Synon.	CCT=Pro	CCC=Pro
					MB21D1_Exon5_2	70	G	R	rs311678	SNP	Coding, Synon.	AAG=Lys	AAA=Lys
WM115	58	female		melanoma	MB21D1_Exon1_1	243	C	A	rs9352000	SNP	Coding, Non-Synon.	ACC=Thr	AAC=Asn
					MB21D1_Exon1_2	11	C	A	rs35629782	SNP	Coding, Non-Synon.	GCG=Ala	GAG=Glu
					MB21D1_Exon1_3	11	T	C	rs9446904	SNP	Coding, Synon.	CCT=Pro	CCC=Pro
					MB21D1_Exon5_2	70	G	A	rs311678	SNP	Coding, Synon.	AAG=Lys	AAA=Lys